Universidade do Minho
Escola de Ciências

Sofia Peixoto Vale

Behavior of contact Lenses incorporating drug-loaded chitosan/hyaluronic acid nanoparticles

Abril de 2025

Behavior of contact Lenses incorporating drug-loaded chitosan/hyaluronic acid nanoparticles
Sofia Peixoto Vale
Uminho | 2025

Sofia Peixoto Vale

Behavior of contact lenses incorporating drug-loaded chitosan/hyaluronic acid nanoparticles

Dissertação de Mestrado
Mestrado em Optometria Avançada

Trabalho efetuado sob a orientação da
Professora Doutora Maria Madalena Cunha Faria Lira
e da
Professora Doutora Elisabete Maria Santos Castanheira Coutinho

Abril de 2025

DIREITOS DE AUTOR E CONDIÇÕES DE UTILIZAÇÃO DO TRABALHO POR TERCEIROS

Este é um trabalho académico que pode ser utilizado por terceiros desde que respeitadas as regras e boas práticas internacionalmente aceites, no que concerne aos direitos de autor e direitos conexos.

Assim, o presente trabalho pode ser utilizado nos termos previstos na licença abaixo indicada.

Caso o utilizador necessite de permissão para poder fazer um uso do trabalho em condições não previstas no licenciamento indicado, deverá contactar o autor, através do RepositóriUM da Universidade do Minho.

Licença concedida aos utilizadores deste trabalho



Atribuição-NãoComercial
CC BY-NC

https://creativecommons.org/licenses/by-nc/4.0/

ACKNOWLEDGMENTS

Quero fazer um breve agradecimento a todos aqueles que me acompanharam nesta jornada. Em primeiro lugar, aos meus pais e à minha irmã, que, mesmo sem entender muito bem o que eu estava a desenvolver, sempre me ajudaram da melhor maneira.

Às amizades que levo desta universidade, em especial à Mota, à Bárbara, à Sabrina e à Costa. Estes últimos anos não seriam tão bons sem vocês ao meu lado.

Não podia deixar de agradecer à Tun'ao Minho, família que me acolheu e ajudou a tornar esta experiência mais leve e animada.

Um obrigada também às minhas amigas de sempre: Susana, Marta, Guida, Isabel e Much, que sempre me apoiaram e nunca me deixaram ir abaixo.

Às minhas orientadoras, Professora Doutora Maria Madalena Cunha Faria Lira e Professora Doutora Elisabete Maria Santos Castanheira Coutinho, um obrigada por toda a ajuda prestada, disponibilidade, motivação para continuar e paciência também.

Agradeço também ao Sérgio Veloso, que acompanhou de perto o meu trabalho, que me ajudou muito e sempre me motivou.

.

STATEMENT OF INTEGRITY

I hereby declare having conducted this academic work with integrity. I confirm that I have not used plagiarism or any form of undue use of information or falsification of results along the process leading to its elaboration.

I further declare that I have fully acknowledged the Code of Ethical Conduct of the University of Minho.

Behavior of contact lenses incorporating drug-loaded chitosan/hyaluronic acid nanoparticles

ABSTRACT

Current treatments for eye disease present significant limitations, such as low drug bioavailability, adverse effects, and patient discomfort. This study aims to evaluate the potential of contact lenses (CLs) embedded with chitosan/hyaluronic acid (Ch/HA) nanoparticles (NPs) loaded with methotrexate (MTX) for use as a sustained ocular drug delivery platform.

MTX-loaded NPs, obtained by the ionic gelation method, were characterized in terms of particle size zeta potential, stability, drug encapsulation efficiency, drug loading capacity, and release profile. Three different materials of silicone-hydrogel CLs were tested: Senofilcon A (Johnson & Johnson), Delefilcon A (Alcon) (daily disposable) and Lehfilcon A (Alcon) (monthly disposable). The CLs were immersed in the solution of drug-laden Ch/HA NPs for two days at a temperature at 4ºC. Before and after this procedure, the CLs' refractive index (RI), water content (WC), and UV/visible transmittance were measured and chemically characterized by FTIR.

The NPs obtained in this study were stable at 4 °C, negatively charged, with hydrodynamic diameters of 284 ± 14 nm (at pH 7.4), low polydispersity, and high MTX encapsulation efficiency (97 ± 1.34%) and drug loading capacity (60 ± 4.49%). NPs adsorption efficiency onto CLs was approximately 96%. After 24 hours, Delefilcon A and Senofilcon A released 22% and 13% of MTX, respectively, and Lehfilcon A released 64% after 30 days, showing sustained release profiles. No significant changes were observed in RI and WC for Lehfilcon A and Delefilcon A CLs, while Senofilcon A showed significant alterations ($p \leq 0.01$). All CLs demonstrated UV/visible transmittance above 85%, except Delefilcon A, which reached a maximum value of 85%. No structural changes were found in the chemical composition of the CLs. In conclusion, Ch/HA NPs enable sustained MTX release from Lehfilcon A and Delefilcon A CLs. These results support the potential of NPs-loaded CLs as a promising platform for future sustained ocular drug delivery system.

Keywords: Chitosan, Contact lenses, Controlled release, Drug Delivery, Hyaluronic Acid, Nanoparticles.

Comportamento de lentes de contacto na incorporação de nanopartículas de quitosano/ácido hialurónico carregadas com fármaco

RESUMO

Os tratamentos atuais utilizados para as doenças oculares apresentam limitações significativas, como baixa biodisponibilidade do fármaco, efeitos adversos e desconforto para o paciente. Este estudo tem como objetivo avaliar o potencial de lentes de contacto (LC) incorporando nanopartículas (NPs) de quitosano/ácido hialurónico (Ch/HA) carregadas com metotrexato (MTX) para entrega sustentada de fármacos em doenças oculares. As NPs carregadas com MTX, obtidas por gelificação iónica, foram caracterizadas em relação ao tamanho, e potencial zeta, estabilidade, eficiência de encapsulamento do fármaco, capacidade de carga do fármaco e perfil de libertação. Foram estudados três materiais de LC de silicone-hidrogel: Senofilcon A (Johnson & Johnson) e Delefilcon A (Alcon) (diárias) e Lehfilcon A (Alcon) (mensal). As LC foram imersas na solução de NPs carregadas com MTX durante dois dias a 4 ^{o}C. Antes e depois da imersão, as lentes foram analisadas quanto ao índice de refração (IR), o conteúdo em água (CA), transmitância UV/visível e caracterização química por FTIR. Neste estudo obteve-se NPs estáveis a 4 °C, carregadas negativamente, com diâmetros hidrodinâmicos de 284 ± 14 nm (pH 7,4), baixa polidispersividade, elevada eficiência de encapsulamento de MTX (97 ± 1,34%) e capacidade de carga do fármaco (60 ± 4.49%). A eficiência de adsorção das NPs nas LC foi de cerca de 96%. Após 24 horas, as LC Delefilcon A e Senofilcon A libertaram 22% e 13% de MTX, respetivamente, enquanto Lehfilcon A libertou 64% após 30 dias, com perfis de libertação sustentada. Não foram observadas alterações significativas no IR e CA das LC Lehfilcon A e Delefilcon A, enquanto Senofilcon A revelou alterações significativas ($p \leq 0,01$). Valor de transmitância UV/visível nas LC superior 85%, exceto nas Delefilcon A (valor máximo de 85%). A estrutura química das LC não foi alterada. Em conclusão, as NPs de Ch/HA permitem a libertação sustentada de MTX pelas LC Lehfilcon A e Delefilcon A. Os resultados revelam que as LC com incorporação de NPs são promissoras para um futuro sistema de administração sustentada de fármacos oculares.

Palavras-chave: Ácido hialurónico, Entrega de fármacos, Lentes de contato, Libertação controlada, Nanopartículas, Quitosano.

TABLE OF CONTENT

ABSTRACT v

RESUMO vi

GLOSSARY OF TERMS & ABBREVIATIONS ix

LIST OF TABLES xii

1. INTRODUCTION 16

1.1 Aims and hypothesis of the study 18

1.1.1 Problem formulation 18

1.1.2 Hypothesis 18

1.1.3 Goals 19

2. LITERATURE REVIEW 20

2.1 Ocular drug delivery systems 20

2.1.1 Contact lenses as drug delivery systems 21

2.1.2 Nanoparticles-laden CLs 22

2.2 Chitosan/Hyaluronic acid nanoparticles 24

2.2.1 Chitosan 24

2.2.2 Hyaluronic Acid 25

2.2.3 Preparation of Chitosan/Hyaluronic Acid NPs 26

2.3 Methotrexate 27

3. MATERIALS AND METHODS 29

3.1 Study design 29

3.2 Materials 29

3.3 Methods 32

3.3.1 Preparation of nanogels and drug encapsulation 32

3.3.1.1 Synthesis of chitosan/hyaluronic acid nanoparticles 32

3.3.1.2 Stability studies of chitosan/hyaluronic acid nanoparticles 33

3.3.1.3 Preparation of MTX-loaded nanoparticles 34

3.3.2 Preparation of contact lenses with nanoparticles containing drug 35

3.3.2.1 Incorporation of Ch/HA nanoparticles in contact lenses 35
3.3.2.2 Drug incorporation into contact lenses 35
3.3.2.3 Incorporation of MTX-loaded Ch/HA nanoparticles into the contact lenses 35
3.3.3 Drug release assays on contact lenses 35
3.3.4 Characterization of the nanoparticles 36
3.3.5 Contact lenses characterization 38
3.4 Statistical analysis 40
4. RESULTS AND DISCUSSION 41
4.1 Sample characterization 41
4.2 Characterization of prepared nanoparticles 41
4.2.1 Particle Size, PDI and zeta potential 42
4.2.2 Stability studies 43
4.3 Characterization of sample F10 46
4.3.1 Influence of pH on the nanogel 46
4.3.2 Scanning electron microscopy 47
4.4 Characterization of MTX loaded nanoparticles 49
4.4.1 Fourier transform infrared spectroscopy 50
4.4.2 Encapsulation efficiency of MTX in NPs 51
4.5 Incorporation of nanoparticles and MTX into CLs 52
4.5.1 Adsorption of Chitosan/Hyaluronic Acid nanoparticles onto CLs 52
4.5.2 Encapsulation efficiency of MTX in CLs 54
4.6 Drug release tests on contact lenses 55
4.7 Characterization of contact lenses 58
4.7.1 Refractive index and water content 58
4.7.2 Transmittance 60
4.7.3 Fourier transform infrared spectroscopy 63
5. CONCLUSIONS AND FUTURE WORK 68
5.1 Conclusions 68
5.2 Future work 71
6. REFERENCES 72

GLOSSARY OF TERMS & ABBREVIATIONS

Ch	Chitosan
ChNPs	Chitosan nanoparticles
CLs	Contact lenses
D	Diopters
DDS	Drug delivery system
DED	Dry eye disease
DEX	Dexamethasone sodium phosphate
DHFR	Enzyme dihydrofolate reductase
DLS	Dynamic light scattering
EE	Encapsulation efficiency
HA	Hyaluronic acid
HCl	Hydrochloric acid
KF	ketotifen fumarate
LC	Loading capacity
MTX	Methotrexate
nAMD	Neovascular age-related macular degeneration
NLCs	Nanostructured lipid carriers
NPs	Nanoparticles

ODDS	Ocular drug delivery system
PDI	Polydispersity index
pHEMA	poly(2-hydroxyethyl methacrylate)
RA	Rheumatoid arthritis
RI	Refractive index
RPG	Rigid gas-permeable
SEM	Scanning Electron Microscopy
STEM	Scanning transmission electron microscopy
TPP	Tripolyphosphate
WC	Water content

LIST OF FIGURES

Figure 1. Chitosan chemical structure. Taken from Jafernik *et al.* [27] 24
Figure 2. Hyaluronic acid chemical structure. Taken from Valachová *et al.* [9] 25
Figure 3. The electrostatic interactions between Ch and TPP. Adapt from Nguyen *et al*.[35] 26
Figure 4. Schematic representation of the synthesis of Ch/HA nanoparticles (by ionotropic gelation) with the incorporation of MTX. 34
Figure 5. Ch/HA with aggregation: Sample 2 with C_{TPP}(wt%) = 0.05 and C_{Ch}(wt%) = 0.1 (A). Ch/HA with aggregation: Sample 10 with C_{TPP}(wt%) = 0.05 and C_{Ch}(wt%) = 0.067 (B). 41
Figure 6. The hydrodynamic diameter (A) and PDI (B) of the samples F11, F12, F13, F14, and F15 at different temperature storage conditions after 1 week of synthesis at 25°C and 4°C. Control = measurement immediately after the sample synthesis. Error bars correspond to standard deviation. “s” means significant ($p \leq 0.05$); “ns” means non-significant ($p > 0.05$). 44
Figure 7. Hydrodynamic diameters of the samples F10 to F18 for one month at 4°C. 45
Figure 8. SEM (A) and STEM (B) images of Ch/HA nanoparticles, with different magnifications. 47
Figure 9. Histogram of the Ch/HA nanoparticles measured in the STEM images. 48
Figure 10. FTIR spectrum of MTX-loaded Ch/HA nanoparticles. 50
Figure 11. Encapsulation efficiency (EE%) of MTX in Ch/AH NPs (A) and loading capacity (LC%) (B) of MTX in the Ch/HA NPs. 52
Figure 12. Adsorption of Ch/HA nanoparticles previously encapsulated with MTX on CLs for 7 days. Error bars correspond to standard deviation. Mass of NPs in CLs (A); adsorption efficiency (%) (B). 53
Figure 13. Encapsulation efficiency of MTX in CLs. Error bars correspond to standard deviation. “ns” means non-significant ($p > 0.05$), “*” means $p \leq 0.05$, “**” means $p \leq 0.01$, “***” means $p \leq 0.001$. 54
Figure 14. Plot of the release of MTX by the three types of contact lenses in pH 6.0 and pH 7.4. Control = CL with MTX adsorption only. 56
Figure 15. Refractive index and water content of CLs. Control = CL that was not immersed in any solution. Error bars correspond to standard deviation. “ns” means non-significant ($p > 0.05$), “*” means $p \leq 0.05$, “**” means $p \leq 0.01$, and “***” means $p \leq 0.001$. 59
Figure 16. Transmittance spectra of CLs. Control = CL that were not immersed in any solution. 62
Figure 17. Infrared spectrum of the three types of CLs in 3 conditions: CLs with Ch/HA nanoparticles, CLs with MTX, and CLs that were not immersed in any solution (Control). Delefilcon A CLs (A); Senofilcon A (B); Lehfilcon A (C) 65

LIST OF TABLES

Table 1 Manufacturing parameters of the contact lenses used. 30

Table 2. Concentration of TPP and Ch in the 18 nanogel samples. 32

Table 3 Experimental condition design 42

Table 4. Results obtained in the DLS for the nanoparticles of sample 10 at different pH levels. 46

Table 5. Results of the DLS analysis of Ch/HA nanoparticles loaded with three concentrations of MTX (100, 250 and 500 µM) at pH 7.4 and 6.0. 49

1. INTRODUCTION

Ophthalmic drops remain the most widely used method for treating many eye diseases today. However, this administration method has several significant limitations. One of them is the low bioavailability of drugs due to factors such as the limited volume of the eye drop that can be applied onto the ocular surface, allied to rapid elimination of the molecule drugs during the first reflex blinking and via nasolacrimal drainage.[1]

To improve the effectiveness of drug administration in the eye, contact lenses (CLs) have received attention in recent years to serve as a drug delivery system (DDS), particularly soft contact lenses. CL allow for localized, controlled drug delivery with higher bioavailability compared to traditional methods, reducing the amount of drug that reaches systemic circulation, which in turn reduces the risk of unwanted effects.[2]

The addition of nanoparticles (NPs) to CL is a promising approach to improve this system, such as prolonging the drug release time by enhancing solubility, absorption, and bioavailability and it can be used in targeted drug delivery to specific cells, tissues, or organs, which reduces the drug dosage, reducing side effects and toxicological reactions.[3]

Methotrexate (MTX) is an antifolate metabolite that inhibits DNA synthesis and repair, as well as cellular proliferation. It is used to treat rheumatoid arthritis (RA) and psoriasis as an anti-inflammatory and immunomodulatory agent and to treat malignant tumors and autoimmune diseases as an immunosuppressant.[4,5]

In ophthalmology, MTX has been used in the treatment of various forms of uveitis (anterior, intermediate, posterior, or panuveitis), scleritis, and ocular mucous membrane pemphigoid. MTX is also used in managing advanced proliferative diabetic retinopathy and primary intraocular lymphoma. Additionally, MTX has been employed in treating neovascular age-related macular degeneration (nAMD) resistant to conventional anti-vascular endothelial growth factor (anti-VEGF) therapy and ocular inflammation associated with Behcet's disease.[5]

The use of methotrexate (MTX) in ophthalmology, although effective, is associated with several side effects related to toxicity and varies depending on the route of administration. Treatments with only intravitreal injections avoid systemic effects. However, intravitreal MTX

is associated with many ocular complications, such as sterile endophthalmitis, cataract, keratopathy, glaucoma, maculopathy, optic atrophy, and vitreous hemorrhage.[5] The most common adverse reaction to repeated injections is corneal epithelial damage.[6] Systemic and intravitreal MTX also reported alterations in the quality of tear film, causing dry eye.[7,8]

Hyaluronic acid (HA) is a chemical widely used in ophthalmology, especially in artificial tears to treat dry eye disease (DED), due to excellent biocompatibility and biodegradability that make it a comfortable compound on the ocular surface.[9,10] It has been in high demand in investigations involving the combination of polymers to produce NPs, such as chitosan (Ch). This other natural polymer exhibits antimicrobial properties, good permeability, and mucoadhesiveness, making it an attractive candidate for DDS.[1,11]

The work of Hashad *et al*.[12,13] demonstrates the feasibility of encapsulating MTX in HA-coated Ch NPs, representing a significant advance in the search for more effective and safe forms of administration.

The current study suggests a novel and non-invasive method for MTX ocular delivery by adapting this system for CL administration. While chitosan, with its mucoadhesive and bioadhesive qualities, helps retention on the ocular surface[14], HA's hydrophilic surface stimulates interaction with the tear film and solves the dry eye issues brought on by MTX.[10] In inflammatory or malignant ocular diseases, this technology would enable controlled drug release, lowering systemic toxicity and increasing treatment effectiveness.

1.1 Aims and hypothesis of the study

1.1.1 Problem formulation

Despite the existence of research into CLs as ocular drug delivery systems (ODDS), there is still no safe and stable system available for commercialization.

This study aims to evaluate the potential of CLs embedded with chitosan/hyaluronic acid (Ch/HA) nanoparticles loaded with methotrexate (MTX) for use as a sustained ocular drug delivery platform. Specifically, the work investigates the incorporation efficiency, drug release kinetics, and the impact of this nanoparticle system on the physical and chemical properties of different types of CLs materials. Conventional eye drops are often limited by poor bioavailability, rapid tear clearance, and low patient compliance. As a promising alternative, nanoparticle-laden CLs have emerged as a novel strategy for sustained and controlled drug delivery to the eye.

1.1.2 Hypothesis

Hypothesis 1 – Suitability of CLs

H0: The CLs selected for the study aren't suitable for incorporating and releasing Ch/HA NPs with MTX.

H1: The CLs selected for the study are suitable for incorporating and releasing Ch/HA NPs with MTX.

Hypothesis 2 – Impact on CLs properties

H0: Ch/HA NPs with MTX cause significant changes in CLs properties.

H1: Ch/HA NPs with MTX cause no significant changes in CLs properties.

Hypothesis 3 – Influence of CLs material type

H0: Different CLs materials have significant differences in the incorporation and release profile of MTX.

H1: Different CLs materials have no significant differences in the incorporation and release profile of MTX.

Hypothesis 4 – Overall potential as a drug delivery system

H0: The system of CLs + NPs of Ch/HA with MTX isn't promising for a future ocular DDS.

H1: The system of CLs + NPs of Ch/HA with MTX is promising for a future ocular DDS.

1.1.3 Goals

The main goal of this study is to evaluate the potential alterations in the properties of the CLs after the incorporation of chitosan/hyaluronic acid nanoparticles and methotrexate.

The specific aims are the following:

- Develop nanoparticles based on Ch and HA capable of effectively encapsulating and transporting MTX.
- Determine the suitability of selected CLs for the study for the incorporation and sustained release of Ch/HA NPs with MTX.
- Evaluate the possible changes in the optical, physical, and chemical properties of the CLs after the incorporation of Ch/HA NPs and MTX.
- To compare the different CLs materials regarding the incorporation and release profile of Ch/HA NPs and MTX.

2. LITERATURE REVIEW

2.1 Ocular drug delivery systems

Ocular treatments can be administered intraocularly (inside the eye), periocularly (subtenon or juxtascleral), on the anterior surface of the eye (topical route), systemically, or together with ophthalmic devices. [15]

Eye drops are the most common form of medication prescribed by eye care professionals in the treatment of various ocular conditions. [11] This method is the easiest and least invasive but presents low bioavailability. Due to the precorneal surface area, there is a limited volume that can be applied to the ocular surface, and most of that volume is eliminated during the first reflex blinking and via nasolacrimal drainage because of tear film turnover. Consequently, this absorption by other tissues can lead to undesirable effects and to ineffective treatment results because the residence time on the ocular surface is not enough for the drug to be absorbed properly. To improve the efficacy of drug delivery, high drug concentrations and repeated doses are often required, which can result in side effects.[1]

To overcome these limitations, the creation of contact lenses as a drug delivery system has been studied. A clinically dosed contact lens, by adhering directly to the ocular surface, can increase the bioavailability of the drug and minimize the loss of the medication to the rest of the body. It can also increase the retention time of the medication on the surface of the eye, which is a great advantage over drops, as often 5% less of the drug reaches the anterior chamber.[1]

Most CLs fittings nowadays (50%, statistics from 2023)[16] are made with silicone hydrogel contact lenses, an improved kind of soft contact lenses made from silicone-based polymers and hydrophilic monomers, such as HEMA. The most common use of a soft contact lens therapeutically has been as a bandage contact lens, to provide a protective cover so the cornea will heal or be protected when it gets scratched or has erosion.[17] However, soft contact lenses are already a familiar method for many patients, making them a convenient option for administering medication. Patients accustomed to wearing lenses may find it easier to integrate medication administration into their daily routine.[1]

2.1.1 Contact lenses as drug delivery systems

Contact lenses (CLs) are classified as “hard” and “soft” depending on the material. Hard CLs, often referred to as rigid gas-permeable (RPG) lenses, are durable and oxygen-permeable, unlike the older PMMA lenses, which lacked oxygen permeability. Soft CLs are highly flexible, oxygen-permeable, and typically have a high water content (WC), allowing them to conform quickly to the eye’s shape.[18]

For the function of ocular drug delivery systems (ODDS), soft contact lenses are preferred because of their hydrophilic properties, biocompatibility, and comfort of use.[2] Soft contact lens materials include hydrogels and silicone hydrogels (SiHy). Hydrogels are usually characterized as extensively swollen polymer networks in water. They can integrate active ingredients within their structure because of their high porosities and surface areas. The drug incorporated into a drug delivery hydrogel lens is released into the tear film, allowing it to reach the target tissue.[19]

Hydrogel CLs are mainly made of hydrophilic copolymers like poly(2-hydroxyethyl methacrylate) (pHEMA), while SiHy are primarily composed of silicon-based materials, including PDMS, TPVC, TRIS, and other siloxane macromolecules, resulting in a more hydrophobic polymer matrix, although they also present hydrophilic monomers, such as HEMA, DMA, and NVP.[19]

This material difference has an impact on drug retention and release: for hydrophilic drugs, hydrogel contact lenses reported better results than silicon CLs, and the opposite has been reported for hydrophobic drugs. [20,21]

The commercial soft CLs are widely available, produced on a large scale, and ensure consistency and reproducibility, making them useful for drug release research. The “soak and release” method, based on soaking CLs in drug solution for drug uptake and subsequent release, was widely used due to its simplicity. However, this approach has significant limitations, primarily the low affinity of CLs for most ophthalmic drugs. Drug-lens affinity is crucial: if too high, the drug remains bound and is not released; if too low, it is rapidly released, leading to a short-lived therapeutic effect.[22]

Soluri *et al.*[23] researched the ability of commercial contact lenses to absorb and deliver ketotifen fumarate (KF), an anti-allergy drug. Fourteen commercially available lenses with different materials were investigated, including classic hydrogels, silicone hydrogels, and daily disposable lenses. Results showed that all the tested lenses released clinically relevant amounts of KF, which was greater than the usual 0.025% eye drop administration in a twice-daily dose. However, release was comparatively quick, and not a single lens maintained release for longer than 4 hours. Despite the brevity of the release, the study discovers that commercial lens wear for the delivery of KF is likely feasible in a daily wear mode.[23]

With proper engineering, the correct dosage can be delivered consistently throughout the intended duration of contact lens wear, eliminating the need for frequent dosing or lens changes. In recent years, research has focused on modifying and controlling drug release kinetics to achieve sustained and controlled delivery. [22]

Recent advances in nanotechnology and biomaterial sciences led to the development of complexes such as nanoparticles (NPs) and the incorporation of these into CLs. [24]

2.1.2 Nanoparticles-laden CLs

Nanoparticles are small carriers that are applied to transport medications, nutrition, or other bioactive substances. They are usually between 1 and 1000 nanometers in size. They enhance the targeted distribution, solubility, and bioavailability of nutritional or medicinal substances. They are mostly separated into lipid nanoparticles and polymers. Polymer-based nanoparticles are colloidal particles made from natural or synthetic polymers, and these can be tailored to respond to environmental triggers like pH or temperature. They include forms like nanospheres, micelles, vesicles, and dendrimers. These systems offer good stability, controlled release, and surface modification capabilities.

Liposomes, solid lipid nanoparticles (SLNs), nanostructured lipid carriers (NLCs), and nanoemulsions are examples of lipid-based nanoparticles. They can include both hydrophilic and hydrophobic substances and are highly biocompatible. The capacity of lipid carriers to preserve and release active components gradually makes them particularly intriguing for use in food and medicinal applications.[25,26]

Compared to lipid-based nanoparticles, polymer-based nanoparticles have several advantages. Because of their increased chemical and physical stability, they are more resilient to temperature and pH variations in the environment. Long-term treatments benefit from their structure, which permits controlled and sustained drug release. Furthermore, polymer NPs are incredibly adaptable and simply surface-modifiable to target tissues or cells. They can also be used to transport a variety of therapeutic substances, including proteins, genetic materials, and hydrophilic and hydrophobic medications. Polymer NPs offer superior protection and delivery efficiency because they are less likely to prematurely leak drugs than lipid-based carriers.[26]

The biological activity of NPs, such as phagocytosis, circulation time, and in vivo diffusion, is influenced by their shape. Non-spherical NPs, despite being less commonly studied, can offer unique advantages in vascular transport and biodistribution compared to spherical ones.[27]

Surface charge and hydrophobicity also play key roles in their biological behavior. While hydrophilic materials reduce immune system clearance, hydrophobic ones enhance tissue penetration. Thus, combining both properties in specific ratios may optimize in vivo stability and targeting efficiency.[27]

In this ocular drug delivery system, nanoparticles are embedded in the matrix of silicone-hydrogel contact lenses, so a drug needs first to diffuse through the nanoparticle, reach the contact lens matrix, and then diffuse through the CLs matrix to reach the target. Research indicates that this method allows a gradual release of the drug, with a longer duration of release compared to the use of NPs or CLs matrix alone.[28] By encapsulating the NP carriers within the CLs matrix, it is also possible to increase the biocompatibility of the NP carriers, stop the NPs from moving away from their target, and reduce the amount of drug metabolism caused by the enzymes found on the tear/corneal surface.[29]

2.2 Chitosan/Hyaluronic acid nanoparticles

2.2.1 Chitosan

Chitosan (Ch) is a linear amino polysaccharide derived from chitin, the main component of shells of crustaceans, insects, and microorganisms, representing the second most abundant natural polymer on earth after cellulose.[27]

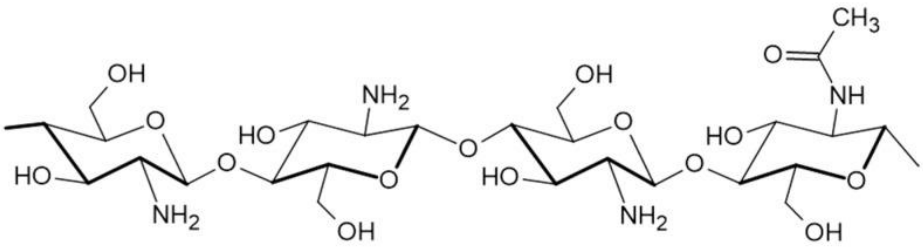


Figure 1. Chitosan chemical structure. Taken from Jafernik *et al.* [27]

Natural polymers are considered more biocompatible and mucoadhesive compared to synthetic polymers, and Ch is one of them. The electrostatic interaction between its positively charged amino groups and the negatively charged mucin residues in the mucosal layer is the reason for its mucoadhesive nature. Hydrophobic interactions and hydrogen bonding also improve the adhesion to mucosal surfaces, such as the surface of the eye. This property increases the time of NPs, improves bioavailability, and reduces the frequency of drugs administered for the effectiveness of therapy. [14]

Ch is also considered a paracellular permeability enhancer due to its ability to reversibly open the tight junctions between epithelial cells present on the cornea, improving drug absorption and therapeutic efficacy.[30]

Chitosan NPs (ChNPs) are often synthesized via ionic gelation techniques using sodium tripolyphosphate as a crosslinker.[31] The ocular retention period of the loaded pharmaceuticals or the ocular penetration of the chitosan NPs can be extended by the crosslinking, which can also lower the initial burst and increase the ocular bioavailability of the medications.[29]

This natural polymer possesses excellent antimicrobial properties.[32] Recent literature reports that chitosan-based NPs can promote antimicrobial and anti-inflammatory activity as well as wound healing.[33]

2.2.2 Hyaluronic Acid

Hyaluronic acid (HA), also known as hyaluronan, is a non-sulfated glycosaminoglycan widely present in various body tissues and organs, like the vitreous body. Its primary structure (**Figure 2**) comprises repeating disaccharide units of N-acetylglucosamine and D-glucuronic acid, connected by β-1,4 and β-1,3 glycosidic bonds, resulting in a linear, negatively charged, water-soluble, and biodegradable polymer.[34]

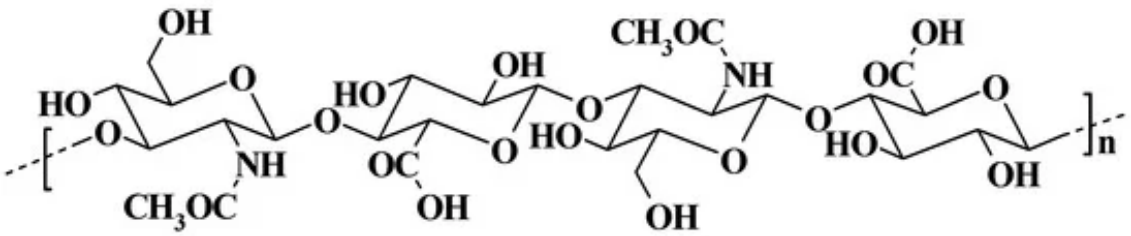


Figure 2. Hyaluronic acid chemical structure. Taken from Valachová *et al.* [9]

This natural polysaccharide is known for its remarkable ability to retain water, which gives it viscoelastic properties, making it valuable in medical applications, including drug delivery systems. In aqueous solutions, the viscosity of HA depends on its molar mass, pH, ionic strength, concentration, and shear rate. Its biocompatibility, biodegradability, and non-immunogenic nature further enhance its suitability for therapeutic use. Chemical modifications, such as cross-linking, improve HA's mechanical stability and extend its residence time in vivo, which is particularly beneficial for sustained drug delivery. [9]

Hyaluronic acid possesses anti-toxic, anti-inflammatory, lubricating, and antioxidant properties at the surface of the eye. Most of the examined literature found that HA, as an active ingredient in artificial tears, is a safe and effective treatment for DED, improving both signs and symptoms at concentrations ranging from 0.1% to 0.4%.[10]

2.2.3 Preparation of Chitosan/Hyaluronic Acid NPs

The ionotropic gelation resulted in the most used method for the preparation of ChNPs (chitosan nanoparticles). This technique requires simple, easy-to-find, and inexpensive materials and equipment, so it can be done easily, mildly, and quickly in normal laboratories.[27]

Ionic interaction occurs between the positively charged amino groups of Ch and anionic cross-linker molecules, generally tripolyphosphate (TPP). There are two primary interactions: H-link, interaction of O^- and NH_3^+ in the same plane, and T-link, interaction of nonbridging oxygen atom and NH_3^+ in different planes (**Figure 3**). In this process, two aqueous solutions, one containing the polycationic polymer and the other consisting of TPP, are mixed according to a specific Ch:TPP w/w ratio, which determines the size and the surface charge of the resulting ChNPs. The Ch concentration, Ch molecular weight, pH, and stirring also influence the formation of NPs.[35]

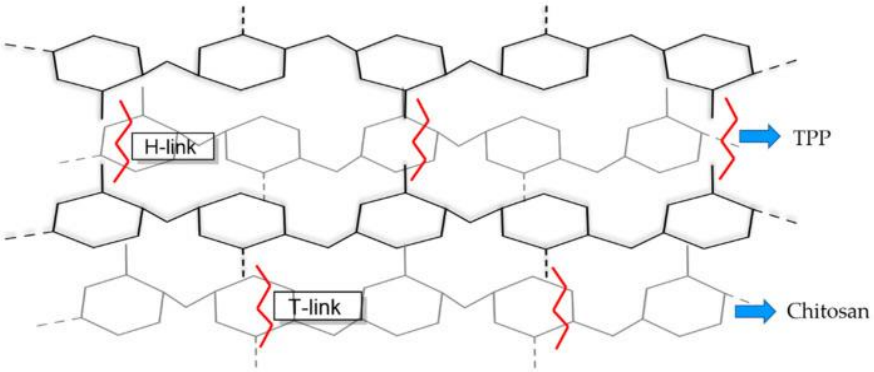


Figure 3. The electrostatic interactions between Ch and TPP. Adapt from Nguyen *et al.*[35]

Chitosan nanoparticles have a positive charge due to the presence of protonated amino groups (NH_3^+). Hyaluronic acid is an anionic polymer (negatively charged) due to the presence of carboxylate groups. When HA is added to chitosan NPs, HA binds to the surface of the particles due to electrostatic interactions between the opposite charges. The result is NPs with a negative surface charge, which creates repulsion between the various NPs, helping to keep them dispersed. Therefore, the coating of chitosan NPs with hyaluronic acid results in a more stable dispersion of NPs.[31]

Chemotherapeutic drugs can be loaded onto nanoparticles (NPs) either during their formation or afterward, through incorporation or incubation methods. The efficiency of drug loading depends on the preparation technique and drug properties. Because of their mucoadhesiveness, biocompatibility, biodegradability, and capacity to improve drug stability and bioavailability, ChNPs are especially efficient drug carriers. Both water-soluble and water-insoluble medications can be carried by them. Particle characteristics, drug features, and environmental factors (such as pH and enzymes) can all affect drug release from ChNPs. Diffusion-based release is typically slower and more gradual, whereas surface-bound medicines frequently generate an initial burst release.[27]

2.3 Methotrexate

Methotrexate (MTX) is a synthetic antifolate drug developed in the 1940s and initially used in the treatment of pediatric leukemia. Its mechanism of action involves inhibiting the enzyme dihydrofolate reductase (DHFR), which is essential for DNA and RNA synthesis. Additionally, MTX inhibits the enzyme ATIC, leading to increased extracellular adenosine levels that contribute to its anti-inflammatory and immunosuppressive effects.[4,36]

Because of its many different pharmacological effects, MTX has been used extensively to treat a wide range of illnesses and conditions, such as psoriasis, rheumatoid arthritis, various cancers, and inflammatory diseases like sarcoidosis. In ophthalmology, MTX has been used systemically or intravitreally to treat a variety of ocular diseases, including primary intraocular lymphoma, noninfectious uveitis, Behçet's disease, scleritis, retinitis related to tuberculosis and Epstein-Barr virus, proliferative vitreoretinopathy, and, in refractory cases, neovascular age-related macular degeneration.[5] The typical intravitreal dose used is 400 µg/0.1 mL, although dosing protocols may vary depending on the clinical indication.[4] Oral tablets and injectable versions (subcutaneous, intramuscular, intravenous, and intrathecal) are among the commercially available formulations of systemic MTX. However, there is currently no commercially available intravitreal MTX formulation specifically designed for ophthalmology. Its application in eye diseases is still off-label and mostly limited to clinical research or specific hospital environments.[4]

One major issue with MTX treatment is still toxicity. Systemic dosing can cause bone marrow suppression, pneumonitis, hepatotoxicity, nephrotoxicity, and an elevated risk of infections and lymphoproliferative diseases, especially when used over an extended period. Individual sensitivity to these negative consequences may be influenced by genetic factors, such as polymorphisms in the MTHFR and RFC1 genes.[5] Intravitreal MTX can result in local ocular problems such as sterile endophthalmitis, cataract, glaucoma, maculopathy, optic atrophy, vitreous hemorrhage, and keratopathy reported in many studies along with dryness signs[37–39]. In addition, MTX was reported to cause alterations in the quality of tear film, causing dry eye both with systemic and intravitreal administration. [7,8]

The most common adverse reaction to repeated injections is corneal epithelial damage, which is typically reversible with the right management.[4,5] Even though this side effects usually well tolerated, they cause discomfort to the patients.

Jeong *et al*.[40] found that after an average of 5.7 injections and an average duration to onset of 5.7 weeks, the incidence of epitheliopathies was 22.7%. Corneal sheet opacities, central epithelial defects, and superficial punctate erosions were the most frequent clinical findings. After stopping MTX or receiving supportive care, the epitheliopathy was always reversible.

To treat primary intraocular lymphoma and protect against central nervous system involvement, Akiyama *et al.*[6] use a combined therapy using intravitreal methotrexate and systemic high-dose MTX, and adverse events were observed like anemia, anorexia, gastrointestinal problems, and keratitis. Although these problems were resolved, they brought discomfort to patients.[6]

Even though these side effects are usually well tolerated, they cause discomfort to the patients, and Ch/HA NPs incorporated into CLs appear in this work as an ocular drug delivery system for MTX to overcome the undesirable effects of its administration via systemic and intravitreal routes in the treatment of ocular diseases.

3. MATERIALS AND METHODS

3.1 Study design

An observational and cross-sectional study was conducted at the University of Minho, Braga, Portugal, between December 2023 and July 2024. This study did not require evaluation by the ethics committee, nor did it need to comply with the usual requirements for studies involving patients, as it did not involve human participants but only materials.

Dynamic light scattering (DLS) measurements, fluorescence spectroscopy assays, UV/visible transmittance measurements, and the preparation of all solutions were carried out at the Photophysics Laboratory of the Center of Physics (CFUM), School of Sciences. Fourier Transform Infrared Spectroscopy (FTIR) measurements were performed at the FTIR Laboratory of the Center of Chemistry, School of Sciences. Scanning Electron Microscopy in Transmission mode (STEM) images were obtained at SEMAT/UM (Materials Characterization Services, Guimarães). RI (Refractive index) and WC (Water Content) measurements of the contact lenses used were conducted at CEORLab (Clinical and Experimental Optometry Research Lab) at CFUM, School of Sciences.

The first stage of the work involved the preparation of chitosan and hyaluronic acid nanoparticles, analysis of the nanoparticles, and the selection of the best and most stable formulation. In the next step, this formulation was used to remake the nanogel with different concentrations of methotrexate, the drug used in the study. The drug-loaded nanoparticles were analyzed, and the formulation with the highest encapsulation efficiency and loading capacity was selected. In the final stage, the chosen NPs, both with and without methotrexate, were incorporated into the three types of contact lenses used in the study, and their properties and behavior were analyzed.

3.2 Materials

All the materials were carefully cleaned and decontaminated to minimize the risk of sample contamination.

I. Reagents

In this study, a variety of reagents were used to prepare and characterize the materials:

- Tripolyphosphate (TPP)
- Chitosan (Ch)
- Hyaluronic acid (HA)
- Hydrochloric acid (HCl)
- Ultra-pure water
- Methotrexate (MTX)

Tripolyphosphate (TPP) was used as a crosslinking agent to interact with chitosan (Ch), a biopolymer known for its biocompatibility and biodegradable properties. Hyaluronic acid (HA), another biopolymer, was included due to its moisturizing and anti-inflammatory characteristics. Hydrochloric acid was used to adjust pH levels during the preparation process, helping with the dissolution of Ch and ensuring optimal conditions for material stability. Ultra-pure water was utilized as the solvent for the reactions and dilutions, minimizing the presence of impurities. Lastly, methotrexate (MTX), an anti-inflammatory and chemotherapeutic agent already used in the clinical practice, was incorporated to evaluate its release and interaction with the developed materials.

II. Contact Lenses

The three types of Si-Hy contact lenses used, as well as their characteristics, are shown in the table.

Table 1 Manufacturing parameters of the contact lenses used.

Commercial name	**TOTAL30™**	**DAILIES TOTAL1™**	**ACUVUE® OASYS 1-Day with HydraLuxe®**
Manufacturer	Alcon	Alcon	Johnson & Johnson
Material	Lehfilcon A	Delefilcon A	Senofilcon A
Water content (%)	55 (core) ~100 (surface)	33 (core) ~100 (surface)	38

DK/T (-3.00D) units	154	156	121
Central Thickness (mm) (-3.00D)	0.08	0.09	0.085
Base curve (mm)	8.4	8.5	8.5
Diameter (mm)	14.2	14.1	14.3
FDA group	V	V	I
Filter	UV – class I, HEVL	No	UV- class I
Replacement regime	Monthly disposable	Daily disposable	Daily disposable
Contact angle (°)	25	34	50
Surface treatment	No	No	No

All the lenses used in the study had powers ranging from -2.00 to -3.75D, aiming to minimize significant variations in lens thickness that could affect the results. This power range was selected to ensure consistency in measurements and to avoid structural differences between the lenses from influencing the final data analysis.[41]

The CLs selected for this study are among the most recent available on the market, exhibiting high oxygen transmissibility values.

TOTAL30™ CLs are the first and unique monthly contact lenses featuring Water Gradient Technology. These lenses have a 55% water content at the core, which gradually increases towards the outer surface, reaching nearly 100% water content. This is achieved through the presence of hydrogel polymers bound together on the surface, providing great wettability and making the lenses ultra-soft, thus enhancing eye comfort. [42]

TOTAL30™ CLs also incorporate the biomimetic *Celligent*® Technology, allowing the lens to mimic the structure of the ocular face. This is due to the polymeric structure of the lens surface, MPC polymers, which emulate the corneal surface structure. This technology not only creates and maintains the water gradient that ensures surface lubrification and softness but also helps prevent bacterial and lipid deposition. [42]

One of the daily CLs used in this study, the DAILIES TOTAL1™, also features the Water Gradient Technology, with 33% of water content at the core and nearly 100% at the surface. This two-phase contact lens also incorporates SmartTear® Technology, which releases phosphatidylcholine (PC), a natural component of the tear film that helps stabilize the lipid layer to prevent tear film evaporation. The release of this zwitterionic phospholipid occurs through diffusion, based on the concentration of PC in the surrounding tear film. [43]

ACUVUE® OASYS 1-Day with HydraLuxe® CLs introduces the technology *HydraLuxe*, which helps maintain the stability of the tear film on lens surface through a network of molecules that mimic the mucins present in tears. This characteristic reduces friction between the lens and the eye's surface, increasing comfort.[44]

3.3 Methods

3.3.1 Preparation of nanogels and drug encapsulation

3.3.1.1 Synthesis of chitosan/hyaluronic acid nanoparticles

For the preparation of the nanoparticles, three solutions were prepared: one of chitosan (Ch), another of tripolyphosphate (TPP), and another of hyaluronic acid (HA), all with a concentration of 0.1 wt% and with ultra-pure water as the solvent. Hydrochloric acid 1M was added to the chitosan solution to facilitate its dissolution, as chitosan does not dissolve at neutral pH. The concentration of Ch and TPP was varied between the solutions (**Table 2**).

Table 2. Concentration of TPP and Ch in the 18 nanogel samples.

Sample name	C_{TPP} (wt%)	C_{Ch} (wt%)	Sample Name	C_{TPP} (wt%)	C_{Ch} (wt%)
A1 (standard)	0.0025	0.0225	**A10**	0.0025	0.0050
A2	0.0012	0.0225	**A11**	0.0012	0.0050
A3	0.0006	0.0225	**A12**	0.0006	0.0050
A4	0.0025	0.0150	**A13**	0.0025	0.0025

A5	0.0012	0.0150	**A14**	0.0012	0.0025
A6	0.0006	0.0150	**A15**	0.0006	0.0025
A7	0.0025	0.0100	**A16**	0.0025	0.0075
A8	0.0012	0.0100	**A17**	0.0012	0.0075
A9	0.0006	0.0100	**A18**	0.0006	0.0075

A standard sample was then prepared with 0.1 wt% of the solution of Ch and 0.1 wt% of the solution of TPP in a TPP-Ch ratio of 1:9 for 2.5 minutes under magnetic stirring, followed by the addition of solvent in a 1:1 ratio.

Another 17 samples, with a final volume of 4 mL, were prepared with different TPP and Ch concentrations, as shown in table 2.

The resultant nanoparticles (NPs) dispersion was then added dropwise to an equal volume of HA solution (0.1 wt%) under strong agitation (500 rpm) at room temperature (25 ± 1 °C).

3.3.1.2 Stability studies of chitosan/hyaluronic acid nanoparticles

The stability studies of NPs were conducted using DLS to measure the size of the nanoparticles over time as well as the zeta potential and polydispersity index. The measurements were performed with 300 µL of nanogel and 800 µL of pH 7.4 buffer solution. The nanoparticles were evaluated for 1 month, and two storage temperatures were also tested: 4 °C and 25 °C.

3.3.1.3 Preparation of MTX-loaded nanoparticles

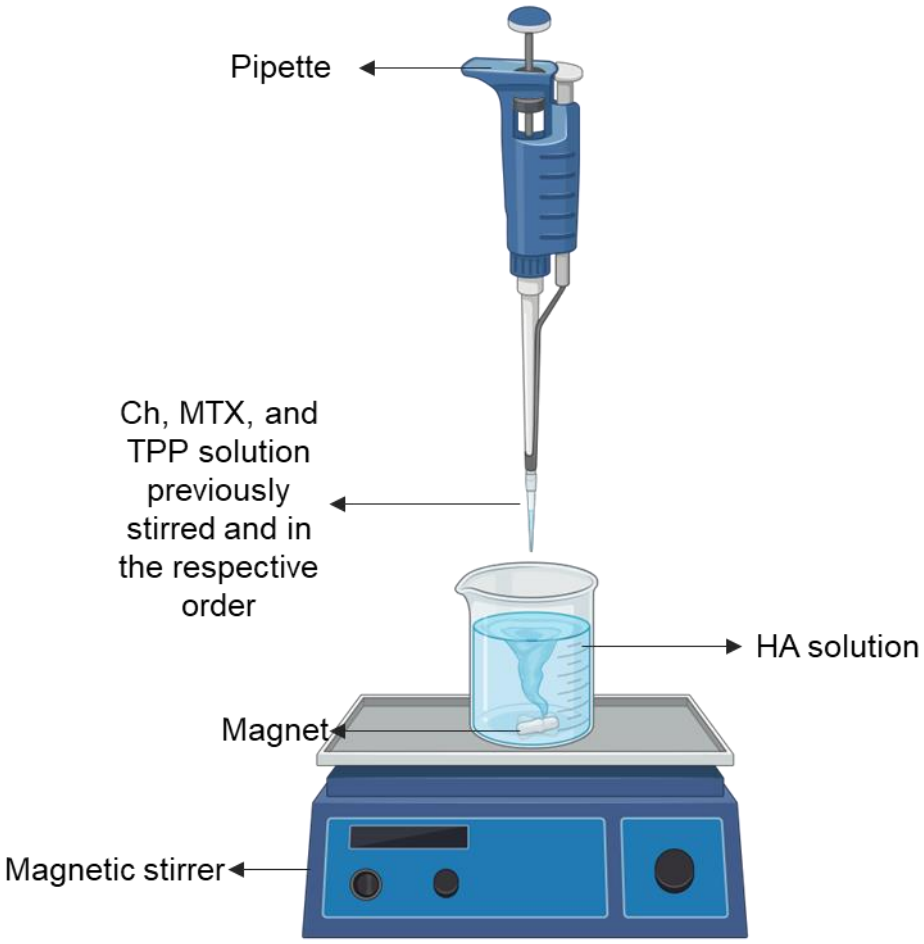


Figure 4. Schematic representation of the synthesis of Ch/HA nanoparticles (by ionotropic gelation) with the incorporation of MTX.

The most stable sample from table 2 was chosen to produce MTX-loaded NPs, satisfying the requirements of reduced hydrodynamic diameter, PDI < 0.2, and a higher negative zeta potential.

For the optimized conditions, MTX diluted in DMSO (10 mM, 25 mM, and 50 mM) was incorporated along with Ch, and from there, the steps were the same as explained in section 3.3.1.1. Through this process, three solutions (2 mL) of chitosan/hyaluronic acid nanoparticles were obtained with MTX loaded at concentrations of 100 µM, 250 µM, and 500 µM.

3.3.2 Preparation of contact lenses with nanoparticles containing drug

In this work, the loading of CLs with drug, or CLs with NPs containing or not encapsulated drug was done by the method of immersion. In each of the following processes, triple trials were carried out for each type of lens used in this study.

3.3.2.1 Incorporation of Ch/HA nanoparticles in contact lenses

The CLs were immersed in a solution of Ch/HA nanoparticles, 0.0575 wt%, for 7 days at a temperature of 4 °C. On the 1st, 2nd, 3rd, and 7th days, a 10 µL aliquot was collected, dried in a weighed aluminum foil, and weighed to study the adhesion efficiency of nanoparticles to contact lenses.

3.3.2.2 Drug incorporation into contact lenses

A solution with MTX diluted in DMSO (50 mM) and ultra-pure water was prepared, with the concentration of 500 µM of MTX. The contact lenses were soaked in the prepared solution for 2 days at a temperature of 4°C.

3.3.2.3 Incorporation of MTX-loaded Ch/HA nanoparticles into the contact lenses

The CLs were soaked in a solution of drug-laden Ch/HA NPs with a concentration of 500 µM of MTX for 2 days at a temperature of 4°C.

3.3.3 Drug release assays on contact lenses

Release assays were carried out after two adsorption tests:

1) Nanoparticles loaded with MTX into CLs.
2) Only drug to CLs.

For each of these situations, the contact lenses were immersed in 1 mL of pH 6 and pH 7.4 buffer solution at room temperature (25 ± 1°C) under agitation of 380 rpm.

I. Daily replacement contact lenses

In this type of lenses, the release tests were carried out for 24 hours from the moment in which they were placed in the buffer solution (0 hours). After 1, 2, 4, 6, 8, and 24 hours, a 200 µL aliquot was removed from the solution, and the fluorescence spectrum was measured. For every 200 µL removed, 200 µL were reposted in the release test, to keep the volume constant.

II. Monthly replacement contact lenses

In this type of lenses, the release tests were carried out for 31 days from the moment they are placed in the buffer solution (0 days). After 1, 4, 5, 6, 7, 11, 12, 13, 19, 25, and 31 days, a 200 µL aliquot was removed from the solution and the fluorescence spectrum was measured. For every 200 µL removed, 200 µL were reposted in the release test, to keep the volume constant.

3.3.4 Characterization of the nanoparticles

I. Dynamic Light Scattering (DLS)

Dynamic Light Scattering (DLS), also known as photon correlation spectroscopy or quasi-elastic light scattering, is an optical technique that uses a laser light source of defined wavelength to measure the size and size distribution of particles and macromolecules in solution. It works by analyzing the time-dependent intensity fluctuations of scattered light caused by the Brownian motion of particles, enabling the calculation of the translational diffusion coefficient and the hydrodynamic radius. [45]

The measurements of particle size, polydispersity index (PDI), and zeta potential of nanoparticles were determined using Anton-Paar DLS, Litesizer™ 500. The samples were diluted with phosphate buffer solution before the analysis and were filtered with an appropriate filter to remove dust. The measurements were performed using an Univette cell, a high-quality reusable cuvette with an optical path of 10 mm. For the determination of the zeta potential, an Omega cuvette was used, with a shape of the capillary tube that resembles an inverted omega and includes two electrodes coated with a 2 µm gold layer to induce an electric field. Scattering angle of 90° was used in all measurements.

II. Fluorescence spectroscopy

This technique was employed due to the fluorescence properties of MTX, enabling the determination of the drug concentration in the solutions and the calculation of the encapsulation efficiency of MTX within the nanoparticles.

Luminescence can be divided into fluorescence and phosphorescence. Fluorescence is the emission of light during the electronic excitation of a sample, while phosphorescence is the emission of light that continues beyond ~10^{-6} seconds after excitation ends. Both are used to study molecular shape, size, and activity, and are commonly grouped under "fluorescence spectroscopy". This technique offers advantages like high sensitivity (< 10^{-12} mol) and specificity. It's particularly responsive to a molecule's microenvironment within ~10 nm and is influenced by molecular motion. [46]

The fluorescence spectra were measured using a Horiba-Jobin-Yvon Fluorolog 3 spectrofluorometer, using a micro-fluorometer cell with a Teflon stopper, UV Quartz, PL 10 mm, Volume 1.40 mL. The excitation wavelength was fixed at 370 nm, and the fluorescence spectra were measured between 450 nm and 480 nm, with an increment of 1 nm and an integration time of 0.2 seconds. With these measurements, the concentration of MTX was determined, which was then used to calculate the drug encapsulation efficiency in the nanoparticles and the amount of drug release by the contact lenses during the release assays.

To obtain a calibration curve of fluorescence as a function of MTX concentration, the following concentrations were used: 0.05, 0.1, 0.20, 0.39, 0.78, 1.56, 3.13, 6.25, 12.5, 25, 50, and 100 µM. Two calibration curves were determined, one with pH 6.0 and the other with pH 7.4, so buffer solution was added to the MTX solution.

To determine the encapsulation efficiency of nanogels, first, 1 mL of nanoparticles solution incorporated with MTX was centrifuged in an Amicon® Ultra Centrifugal Filter, at 4500 rpm for 45 min, to separate the encapsulated drug from the non-encapsulating drug. Then, the fluorescence spectrum of the non-encapsulated drug solution was measured, and the encapsulation efficiency was calculated using equation 1:

$$\boldsymbol{EE}\ (\%) = \frac{(\boldsymbol{Initial\ amount\ of\ drug - amount\ of\ drug\ nonencapsulated})}{\boldsymbol{Initial\ amount\ of\ drug}} \times \mathbf{100}$$ **(Equation 1)**

III. Scanning Electron Microscopy (SEM)

SEM is a surface imaging technique in which an electron beam scans the specimen's surface, interacting with it to generate signals that provide information about the atomic composition and detailed topography of the sample.[47] SEM microscopes can be equipped with detectors to collect electrons transmitted through thin specimens. This scanning mode, which involves collecting transmitted signals, is referred to as scanning transmission electron microscopy (STEM).[48]

These methods reveal the size and shape heterogeneity of the samples, as well as the degrees of aggregation and dispersion.[47] SEM and STEM images were obtained using the NanoSEM-FEI Nova 200 equipment.

3.3.5 Contact lenses characterization

The optical and structural properties of contact lenses were analyzed to measure possible changes after the adsorption of NPs and methotrexate. The characterization techniques were applied to the lenses that were not immersed in any solution (control), CLs with NPs adsorption, and CLs with MTX adsorption.

I. Refractive index and water content

The refractive index and the water content were obtained using the digital automated refractometer CLR 12-70, Index Instruments, Cambridge, UK. The equipment directly measures the RI and has shown valid and accurate readings.[49] With a database of up to 10 different polymer materials, the water content is estimated through an equation, and the value is read directly on the device.[50]

$$\boldsymbol{Watercontent}(\%) = \frac{\boldsymbol{n_1 - n_2}}{\boldsymbol{n_1 - n_s}}$$ **(Equation 2)**

where n_1, n_2, and n_s represent the refractive index of the dehydrated polymer, the contact lenses, and the solution in which the lenses were immersed, respectively.

First, the lens was removed from the blister, and the excess solution from the CLs was taken out with absorbent paper and silicone tweezers. To obtain more reliable results, three measurements per lent were taken, and the average of these results was considered for analysis.

II. Transmittance

The transmittance of the contact lenses was measured using a Shimadzu UV-VIS-NIR spectrophotometer, model UV-3600 Plus.

Initially, a baseline was established on the instrument. The lenses were handled using silicone tweezers, removed from their solution, and any excess liquid was removed with absorbent paper. Measurements on the spectrophotometer were performed with the lens convex surface oriented toward the incident beam, like how it would be placed in the eye, on an appropriate sample holder. The transmittance spectra were plotted as a function of wavelength, between 200 nm and 700 nm.[51]

I. Fourier-transform infrared spectroscopy (FTIR)

Infrared spectroscopy examines the interaction between infrared radiation and matter. When an infrared beam is directed to a sample, the wavelengths absorbed are dependent on the material's molecular vibrations. As a result, by measuring a sample's infrared absorbance, one can extract both chemical and structural information.[52]

There are multiple ways to direct infrared light to samples, and a variety of detectors are available.[52] In this study, Attenuated Total Reflectance Fourier Transform Infrared (ATR FTIR) spectroscopy was used, which involves directing the infrared light towards an interface formed between an infrared transparent material with a high reflection element (IRE, such as a prism made of ZnSe, diamond, silicon, or germanium) and a sample on the surface of the IRE.[52]

FTIR spectroscopy technique coupled to an attenuated total reflectance accessory was used thought the Spectrum Two FT-RI Spectrometer (DTGS Detector), Perkin Elmer. The measurements were taken in the range between 4000 and 400 cm^{-1} using 32 scans and a nominal resolution of 8 cm^{-1}.

3.4 Statistical analysis

To conduct the statistical analysis, the JASP statistical program (version 0.19) was used. The Shapiro-Wilk test with Lilliefors correction was used to evaluate the data distribution's normality and a p-value greater than 0.05 was considered indicative of a normal distribution.

Since the sample data followed a normal distribution, parametric tests were employed. Differences in the means of quantitative variables between independent samples were analyzed using the Independent Samples T-Test when comparing two groups, and the One-Way ANOVA when comparing three or more groups. For multiple comparisons, Tukey's post hoc test was used when the assumption of homogeneity of variances was met, while the Games-Howell post hoc test was applied when this assumption was not met.

4. RESULTS AND DISCUSSION

4.1 Sample characterization

In this work it were used daily replacement CLs (Total 1, Acuvue Oasys with HydraLuxe 1-Day) and monthly CLs (Total 30) **(Table 1)**. The CLs power ranged from -2.00 D to -3.50 D. Given that lens power can influence the outcomes, it was considered as a factor in the analysis to account for potential variations in the results.

4.2 Characterization of prepared nanoparticles

To gain an understanding of the influence of reagents in the formulation of NPs, two variables, chitosan and TPP, were investigated at different concentration levels. A total of 18 different samples were taken, as shown in **Table 2**. Since the HA solution made up half of each sample's volume, each sample had the same concentration of HA, 0.05 wt%.

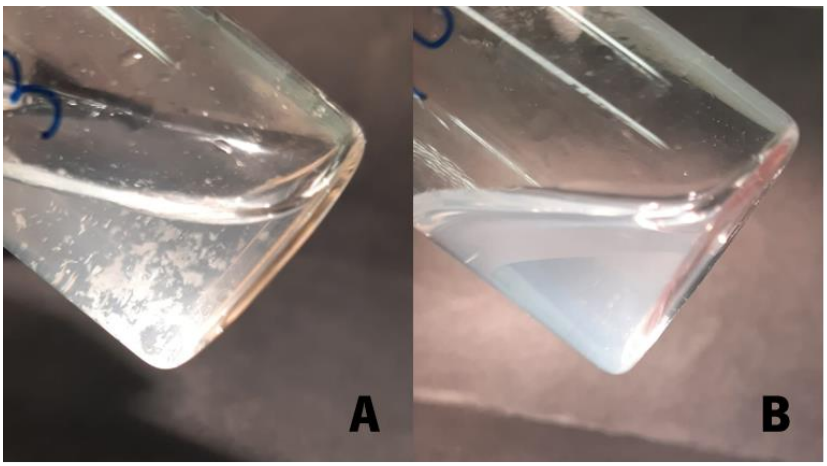


Figure 5. Ch/HA with aggregation: Sample 2 with C_{TPP}(wt%) = 0.05 and C_{Ch}(wt%) = 0.1 **(A)**. Ch/HA with aggregation: Sample 10 with C_{TPP}(wt%) = 0.05 and C_{Ch}(wt%) = 0.067 **(B)**.

The samples 1 to 9 produced aggregates (**Figure 5 A**) when the TPP solution and chitosan were combined with HA. These samples correspond to solutions with a higher concentration of chitosan. On the other hand, the opalescent or milky appearance is the sign of the formation of NPs.[53]

When the concentration of Ch is higher, more protonated amino groups (NH_3^+) will be present in the solution. If the amount of HA (negative charge) is not sufficient to cover these positive charges, the NPs may acquire a less negative, more neutral surface charge. This reduces the electrostatic repulsion between the NPs, leading to aggregation. [54]

4.2.1 Particle Size, PDI and zeta potential

The effect of the selected variables on particle diameter, PDI, and zeta potential of the Ch/HA NPs was determined as shown in **Table 3**. We analyzed samples 10 to 18 using dynamic light scattering (DLS) and was used a 10 mM buffer solution at pH 7.4, which corresponds to the pH of blood.

Table 3 Experimental condition design

Sample	C_{TPP} (wt%)	C_{Ch} (wt%)	Hydrodynamic diameter (nm)	Polydispersity index	Zeta Potential (mV)
F10	0.0025	0.0050	286 ± 14	0.13 ± 0.04	-11.13 ± 0.40
F11	0.0012	0.0050	329 ± 7	0.12 ± 0.05	-7.18 ± 0.09
F12	0.0006	0.0050	230 ± 34	0.19 ± 0.02	-7.53 ± 0.45
F13	0.0025	0.0025	283 ± 35	0.13 ± 0.09	-9.71 ± 0.20
F14	0.0012	0.0025	358 ± 22	0.19 ± 0.03	-9.72 ± 0.12
F15	0.0006	0.0025	373 ± 31	0.12 ± 0.08	-10.32 ± 0.11
F16	0.0025	0.0075	132 ± 3	0.12 ± 0.02	-9.34 ± 0.20
F17	0.0012	0.0075	293 ± 4	0.20 ± 0.04	-7.35 ± 0.14
F18	0.0006	0.0075	274 ± 23	0.17 ± 0.06	-6.38 ± 0.15

Smaller diameters are generally preferred for ocular delivery, as they can more easily penetrate ocular tissues and provide a more controlled release of the drug, and because larger particles cause discomfort and irritation to the eyes. For the NPs to function consistently, a more uniform size distribution is indicated by PDI values below 0.2.[55] Higher negative zeta potential indicates better colloidal stability, preventing the aggregation of nanoparticles.

Based on these parameters and analyzing the **Table 3**, F16 and F10 will be the most suitable samples for transporting ocular drugs. The F16 sample is the one that presents the smallest hydrodynamic diameter of 132 nm, a PDI of 0.12, which indicates a uniform distribution of NPs, and a zeta potential of -9.34 mV, indicating stability.

On the other hand, although the hydrodynamic diameter of F10 is higher than that of F16, it remains small. This sample exhibits a close PDI value of F16 and has higher negative zeta potential, indicating a high degree of stability.

Sample F10 showed an average hydrodynamic diameter of 286 ± 14 nm, a polydispersity index of 0.13 ± 0.04 and a zeta potential of -11.13 ± 0.40 mV. These values are in line with those reported by Kalam *et al*.[54], who observed chitosan nanoparticles coated with hyaluronic acid (formulation F2) with an average size of 385.72 ± 13.18 nm, PDI of 0.178 ± 0.067, and zeta potential of -33.74 ± 3.45 mV. Although the particles developed in this study are slightly smaller in size and less negative in zeta potential, both formulations present PDI below 0.2, reflecting monodisperse distribution, suitable for ocular delivery systems.[55] The difference observed in zeta potential may be related to the degree of coating with hyaluronic acid and the experimental conditions used, such as pH. It is important to note that in the study by Kalam *et al*.[54], all chitosan nanoparticles evaluated were prepared with dexamethasone sodium phosphate (DEX) incorporated from the initial stage of the formulation.

4.2.2 Stability studies

To evaluate the behavior of the nanogels with temperature, the size and polydispersity index of samples stored in different environments was analyzed after 1 week of synthesis. Two samples of each formulation were synthesized, and one of each was stored at a room temperature of 25°C and the other at a lower temperature condition of 4°C. The control measurement was measured immediately after the nanoparticles were prepared.

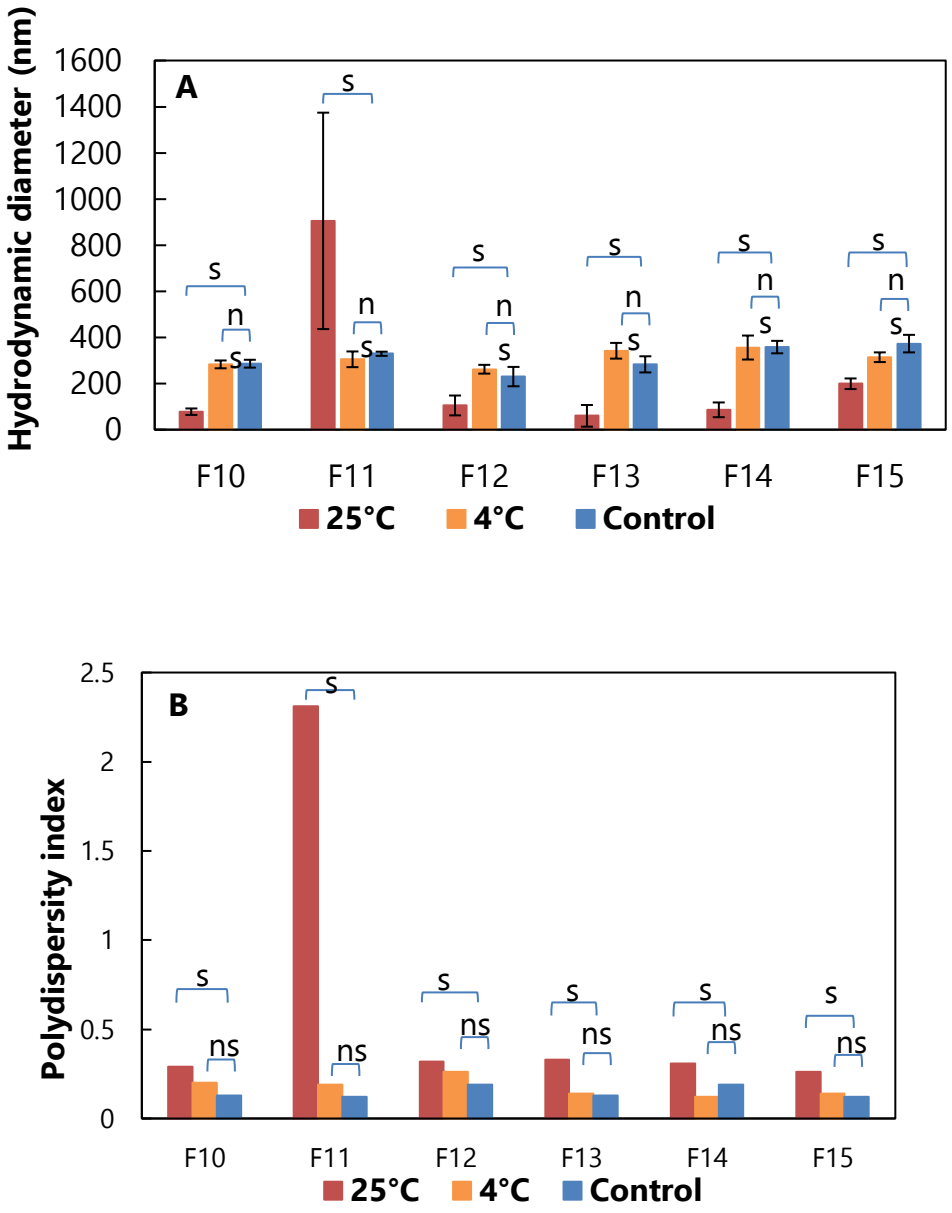


Figure 6. The hydrodynamic diameter (**A**) and PDI (**B**) of the samples F11, F12, F13, F14, and F15 at different temperature storage conditions after 1 week of synthesis at 25°C and 4°C. Control = measurement immediately after the sample synthesis. Error bars correspond to standard deviation. "s" means significant ($p \leq 0.05$); "ns" means non-significant ($p > 0.05$).

Except for sample 11, all samples decreased in hydrodynamic diameter when stored at 25°C, and all samples increased their polydispersity index also at 25°C (**Figure 6**). These variations are indicative of aggregation, as nanoparticles can form smaller, more compact, and

denser aggregates compared to individual NPs. The increase in the PDI value indicates greater variability in the size of the nanoparticles.

In every sample, there are statistically significant variations between the 25°C condition and the control ($p \leq 0.05$). Since these differences do not exist between 4°C and the control, it is concluded that it is more suitable to store the samples at 4°C without significantly changing the characteristics such as size and homogeneity.

A study of the size of nanoparticles as a function of time was also carried out. For this purpose, the 9 nanoparticle samples (F10-F18) were measured, using DLS, for 1 month and stored at 4°C.

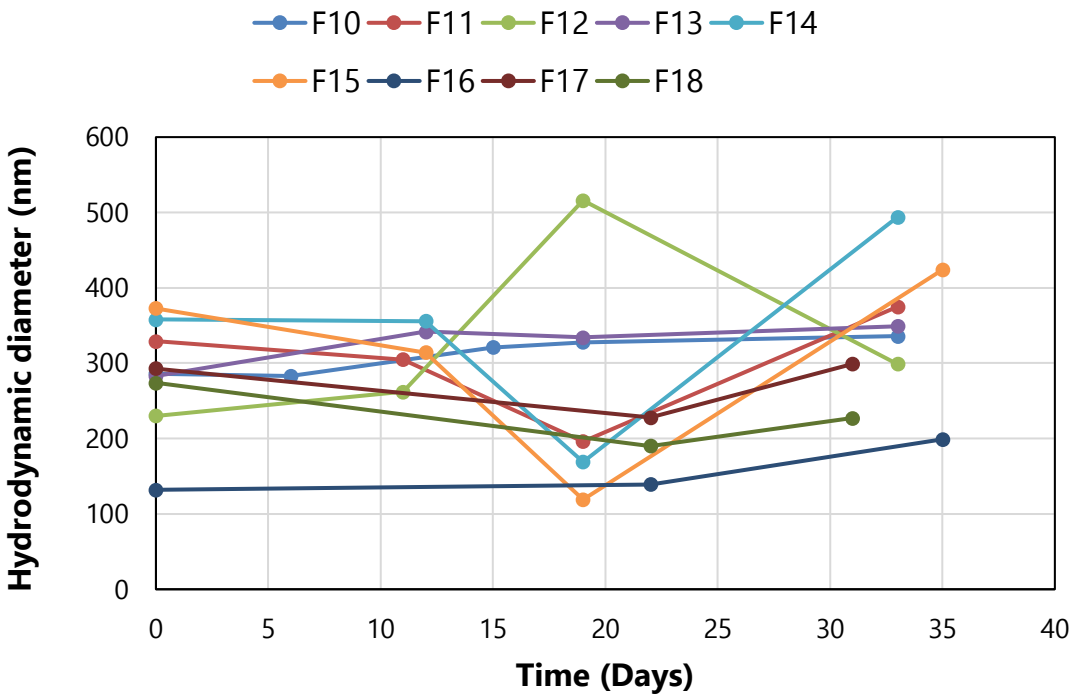


Figure 7. Hydrodynamic diameters of the samples F10 to F18 for one month at 4°C.

Analyzing **Figure 7** it was noticed that the sample that had the least size fluctuations for one month was sample 10. This sample was chosen as being the most stable. These stability results agree with the polydispersity index and zeta potential parameters that can be observed in **Table 3** for sample 10.

4.3 Characterization of sample F10

4.3.1 Influence of pH on the nanogel

The F10 sample was evaluated in buffer solutions (10 mM) of pH 6.0 and 7.4 using DLS, and it was possible to obtain the results on **Table 4**.

Table 4. Results obtained by DLS for the nanoparticles of sample 10 at different pH values.

Buffer solution	Hydrodynamic diameter (nm)	Polydispersity index	Zeta potential (mV)
pH 7.4	286 ± 14	0.13 ± 0.04	-11.13 ± 0.40
pH 6.0	153 ± 7	0.08 ± 0.02	-16.98 ± 0.69

Regarding the size of the NPs, it is observed to be smaller at pH 6.0 compared to pH 7.4, with a statistically significant difference ($p \leq 0.05$). Therefore, the hydrodynamic diameter tends to increase as the pH increases. In both conditions, a polydispersity index below 0.20 was obtained. However, at pH 6.0, the value 0.08 is significantly lower and ≤ 0.1, indicating highly monodisperse NPs.[56] A statistically significant difference ($p \leq 0.05$) is also found in the comparison of zeta potential measurements. The surface charge of the NPs is more negative at pH 6, which reveals greater colloidal stability.

These differences in the values of diameter and surface charge can be justified by the influence of pH on the protonation of Ch and the electrostatic interactions between Ch and HA. In an acidic pH, Ch becomes more protonated with more positive charge, increasing the attractive forces between the molecules.[57] As a result, the NPs become more compact, with less size variability and greater negative surface charge.

It is concluded that pH has a significant influence on the hydrodynamic diameter, polydispersity, and zeta potential of Ch/HA NPs. The choice of a slightly more acidic pH is more appropriate for preserving the stability of the NPs and lowering their propensity to aggregate.

For maximal ocular comfort, an ideal pH for ophthalmic preparations is 7.2 ± 0.2 and, at this pH, the Ch/Ha NPs have also suitable properties for the intended application. However, the eye can tolerate slightly altered pH values, which can be buffered by tears to bring the pH back to physiological levels following ocular instillation.[33]

4.3.2 Scanning electron microscopy

Through this technique, scanning electron microscopy (SEM) and its use in transmission mode (STEM), it was possible to characterize the morphology and size of Ch/HA NPs.

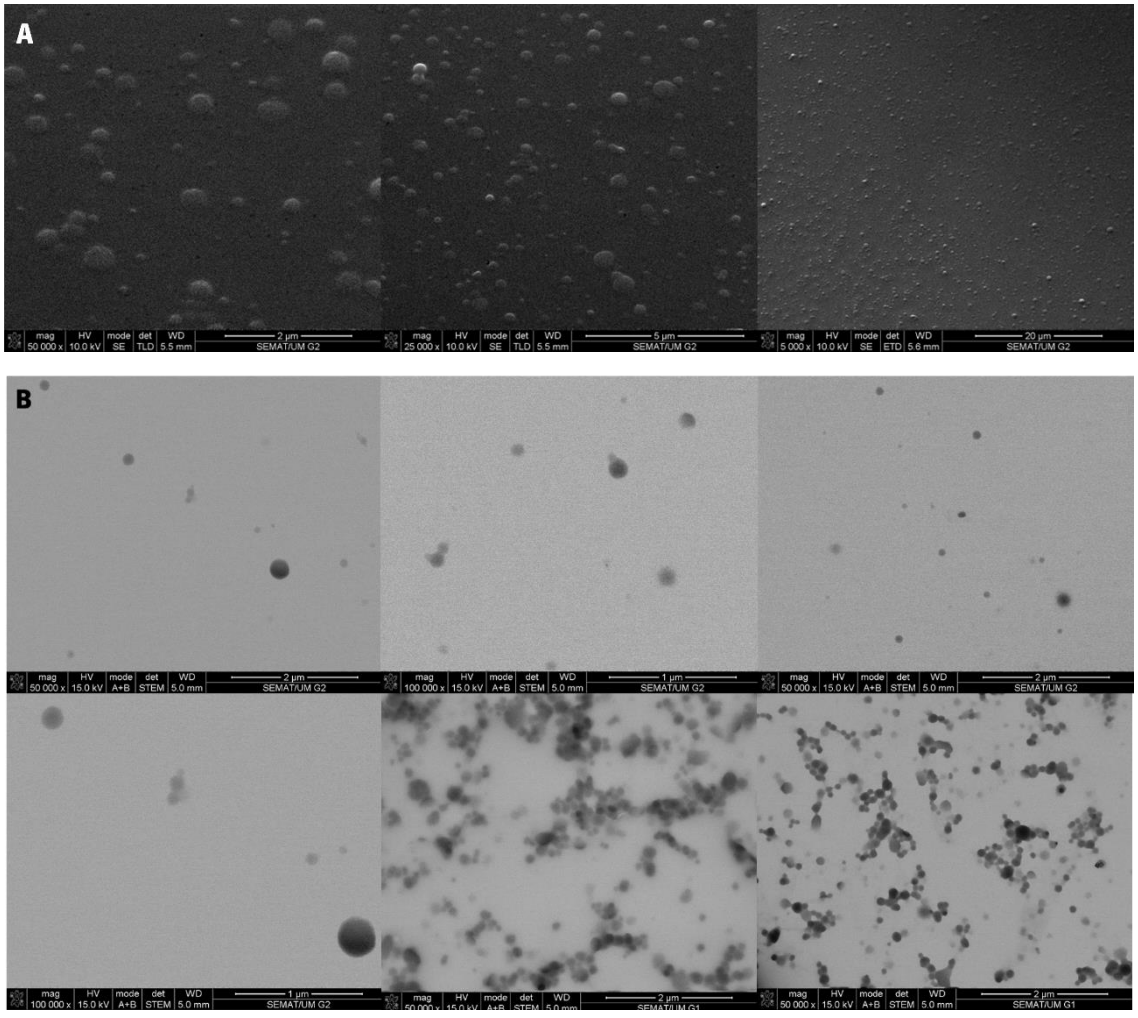


Figure 8 SEM **(A)** and STEM **(B)** images of Ch/HA nanoparticles, with different magnifications.

SEM images (**Figure 8 A**) reveal that the NPs exhibit a spherical shape and are homogeneously distributed across the surface. The varying magnifications highlight

differences in particle sizes and confirm the presence of nanoscale structures. The STEM images (**Figure 8 B**) provide further insights into nanoparticle dispersion and individual morphology. NPs appear well-defined and primarily spherical, although some degree of aggregation is observed. This aggregation can be attributed to the electrostatic interactions between nanoparticles, which is a common phenomenon in polyelectrolyte-based nanoparticles such as chitosan-hyaluronic acid systems, or the sample was not well dispersed before preparation for drying.

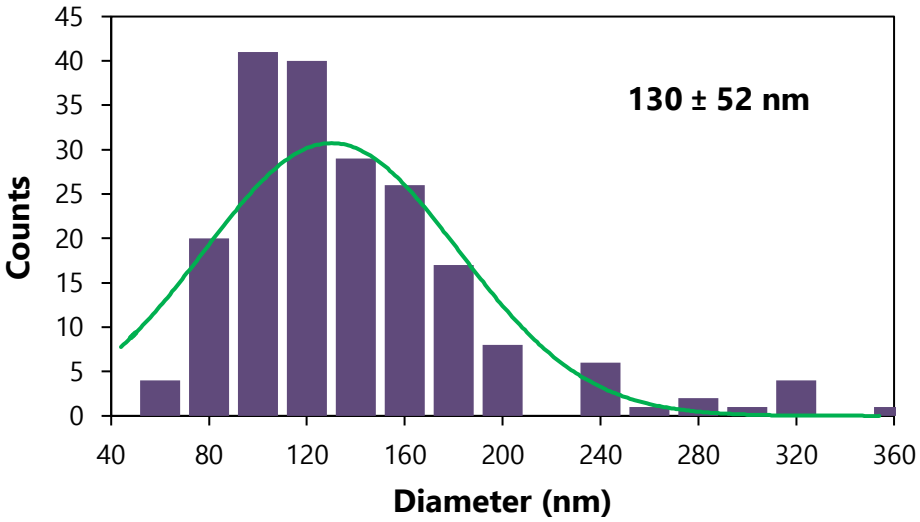


Figure 9. Histogram of the Ch/HA nanoparticles measured in the STEM images.

With the help of the ImageJ program, the nanoparticles present in the previous images (**Figure 8**) were measured, and the histogram shown in **Figure 9** was created. The size distribution histogram indicates that the nanoparticles exhibit a size range between approximately 80 nm and 250 nm, with a peak around 120-140 nm, and have average diameters of 130 ± 52 nm. The observed distribution suggests moderate polydispersity, which is expected in ionotropic gelation synthesis methods. [58]

Using the DLS technique, a size of 286 ± 14 nm was obtained for the same sample. DLS measurements provide larger size measurements when compared to STEM. While DLS measures the hydrodynamic diameter, which includes not only the core nanoparticle size but also the surrounding solvent layer and any adsorbed molecules, STEM provides physical diameter by directly imaging the dry particles, without considering hydration or aggregation

effects. DLS is highly sensitive to particle aggregation in solutions. If the nanoparticles cluster together, the scattered light signal gives an average size that can be significantly larger than the individual particles observed in SEM.[59]

Despite the variation in size, the nanoparticles remain within an optimal range for drug delivery.

4.4 Characterization of MTX loaded nanoparticles

Three different concentrations of MTX were employed in the synthesis of Ch/HA NPs loaded with MTX: 100, 250, and 500 µM. According to **Table 5**, there are no statistically significant differences ($p > 0.05$) in the size parameter except between 0 µM and 250 µM concentrations at pH 7.4.

Table 5. Results of the DLS analysis of Ch/HA nanoparticles loaded with three concentrations of MTX (100, 250, and 500 µM) at pH 7.4 and 6.0.

C (µM)	pH	Hydrodynamic diameter (nm)	PDI	Zeta potential	Statistical significance
0	7.4	286 ± 17	0.13	-11.13	NA
	6.0	153 ± 8	0,08	-16,98	NA
100	7.4	339 ± 20	0,14	-11,08	ns ns ns
	6.0	146 ± 4	0,08	-14,1	ns ns $p \leq 0.05$
250	7.4	218 ± 24	0,21	-7,97	$p \leq 0.05$ ns ns
	6.0	138 ± 5	0,12	-0,04	ns ns $p \leq 0.001$
500	7.4	284 ± 16	0,13	-8,53	ns ns ns
	6.0	180 ± 22	0,1	-15,82	ns ns ns

NA: not applicable

ns: non-significant ($p > 0.05$)
Statistical significance: refers to the difference between the control group (0 µM) and each concentration at the respective pH.

Regarding polydispersity, it's observed that there are no statistically significant differences between the various drug concentrations ($p > 0.05$) and the control group, the Ch/HA NPs without MTX, at different pH values.

At pH 6, there are statistically significant variations in the zeta potential between two of the drug concentrations and the 0 µM concentration. This difference is higher between concentrations 0 µM and 250 µM ($p \leq 0.001$) than between concentrations 0 µM and 100 µM ($p \leq 0.05$), and as this value approaches the neutral value of surface charge, it may be strongly linked to measurement problems related to DLS.

It is observed that drug encapsulation does not cause a significant impact on size, polydispersity, and surface charge in NPs.

4.4.1 Fourier transform infrared spectroscopy

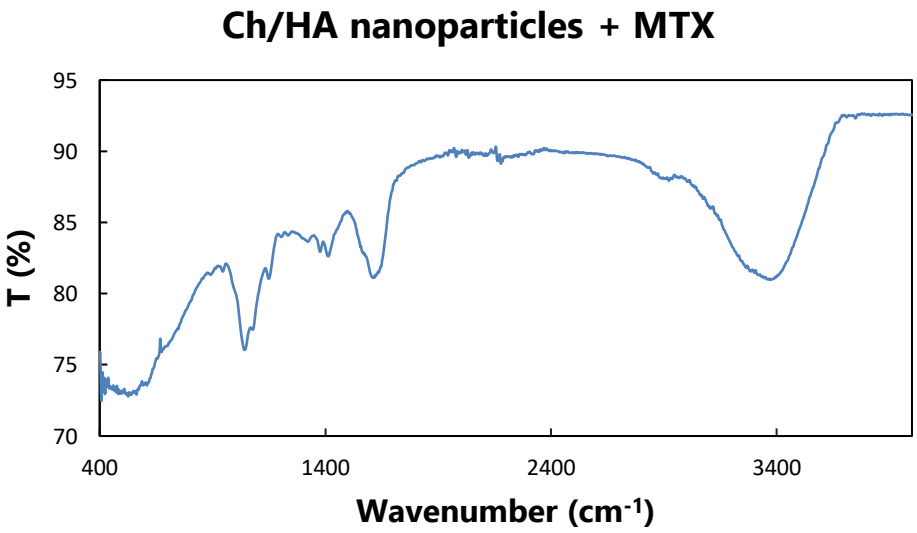


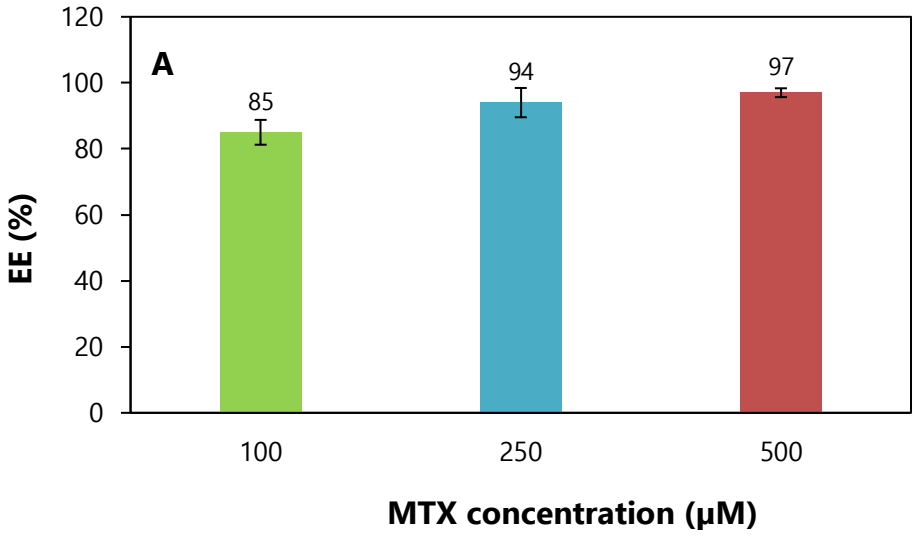
Figure 10. FTIR spectrum of MTX-loaded Ch/HA nanoparticles.

The FTIR spectrum of MTX-loaded Ch/HA nanoparticles **(Figure 10)** displays specific absorption bands that match the functional groups of the materials involved. A wide band near 3,400 cm^{-1} is linked to O–H and N–H stretching vibrations, showing a strong hydrogen

bond between chitosan, MTX, and hyaluronic acid with its carboxylic groups. The existence of MTX within the nanoparticles is indicated by the presence of peaks near 1650 cm^{-1} and 1550 cm^{-1}, which correspond to C=O stretching (amide I) and N–H bending (amide II). The C–O or P=O vibrations of the chitosan and TPP crosslinking, respectively, and the symmetric stretching of HA COO^- are linked to additional bands observed at 1400–1300 cm^{-1} and 1100 cm^{-1}.[12,35,60] These findings demonstrate that each element was successfully incorporated into the nanoparticle system without exhibiting detectable chemical deterioration.

4.4.2 Encapsulation efficiency of MTX in NPs

The encapsulation efficiency (EE%) of MTX in the NPs was analyzed using fluorescence spectroscopy (**Figure 11 A**). The three quantities of the drug (100, 250, and 500 µM) were evaluated without the use of buffer solution.



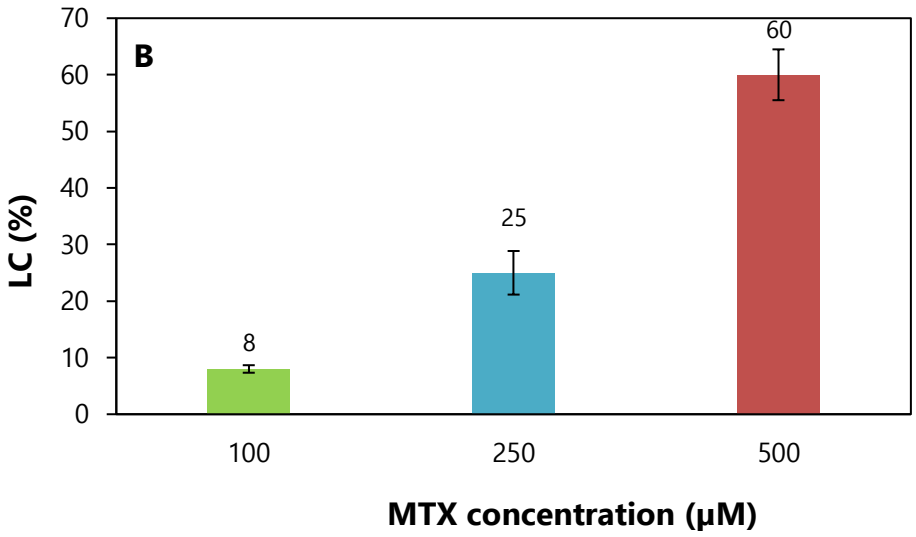


Figure 11. Encapsulation efficiency (EE%) of MTX in Ch/AH NPs **(A)** and loading capacity (LC%) **(B)** of MTX in the Ch/HA NPs.

For all the MTX concentrations, the EE% exceeds 80%, and the 500 µM concentration has the highest EE% value of 97 ± 1.34 %.

On the other hand, **Figure 11 B** shows that the drug loading capacity (LC%) at concentration of 500 µM (60 ± 4.49 %) is significantly larger than at concentrations of 100 µM and 250 µM, where the LC% is 8 ± 0.66 % and 25 ± 3.85 %, respectively. Thus, the ideal concentration of MTX would be 500 µM.

4.5 Incorporation of nanoparticles and MTX into CLs

4.5.1 Adsorption of Chitosan/Hyaluronic Acid nanoparticles onto CLs

During seven days of incorporation of NPs in the two types of CLs, the results shown below were obtained (**Figure 12**), considering that the initial mass of NPs was 19.6 mg.

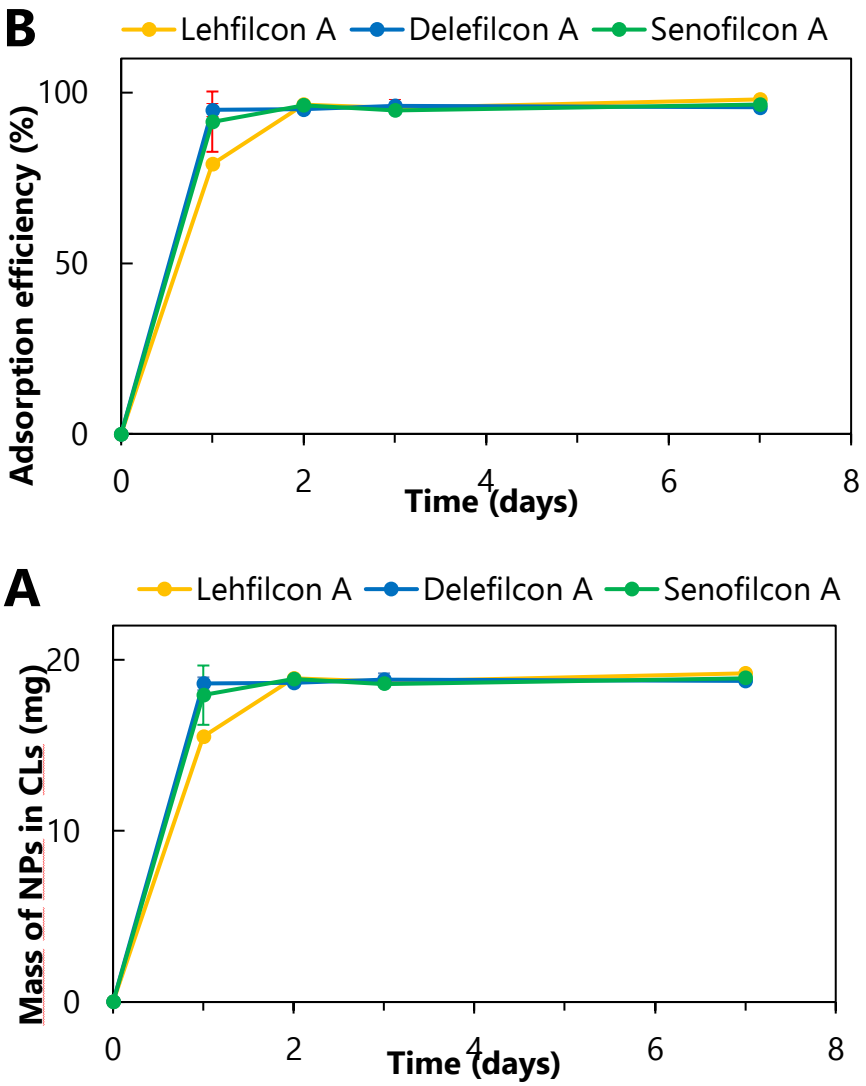


Figure 12. Adsorption of Ch/HA nanoparticles previously encapsulated with MTX on CLs for 7 days. Error bars correspond to standard deviation. Mass of NPs in CLs **(A)**; adsorption efficiency (%) **(B)**.

By analyzing graphs A and B in **Figure 12**, it is possible to perceive an abrupt increase in the mass of NPs that adhered to the CLs on the 1st day with values of 15.5 ± 0.6 mg, 18.6 ± 0.4 mg, and 17.9 ± 1.73 mg with adsorption efficiencies of 79 ± 3%, 95 ± 2%, and 91 ± 9% for Lehfilcon A, Delefilcon A, and Senofilcon A, respectively. On the second day, the monthly lens (Lehfilcon A) had an increase in the mass of adsorbed NPs to 18.91 ± 0.2 mg associated with an efficiency of 96 ± 1 %. The two daily lenses had a slight increase with a mass of 18.64 ± 0.1 mg and 95 ± 0.6% efficiency for Delefilcon A and a mass of 18.87 ± 0.1 mg with 96 ± 0.6 % efficiency for the Senofilcon A lens. On the third and seventh days, the value remained constant for all CLs. We can conclude that the CLs only need two days to adsorb 19.6 mg of

NP mass since on the second day the lenses already showed an adsorption efficiency close to 100%.

There were no differences in the adsorption behavior of Ch/HA nanoparticles on the three CLs materials despite their different characteristics and compositions. They have similar central thicknesses, although their water contents are quite different, as can be seen in **Table 1**. Lehfilcon A and Delfilcon A CLs were specifically designed to resist protein deposition[42,43], which would typically suggest a lower adsorption efficiency for nanoparticles. However, all three CLs exhibited similarly high nanoparticle adsorption efficiencies. This unexpected result may be attributed to differences in the interaction mechanisms between nanoparticles and lens surfaces compared to those of protein adsorption, highlighting the distinct physicochemical properties governing nanoparticle attachment.

4.5.2 Encapsulation efficiency of MTX in CLs

To test the efficiency of drug incorporation into CLs, two processes were compared: drug encapsulated in Ch/HA NPs and the isolated drug, and the results are in **Figure 13**.

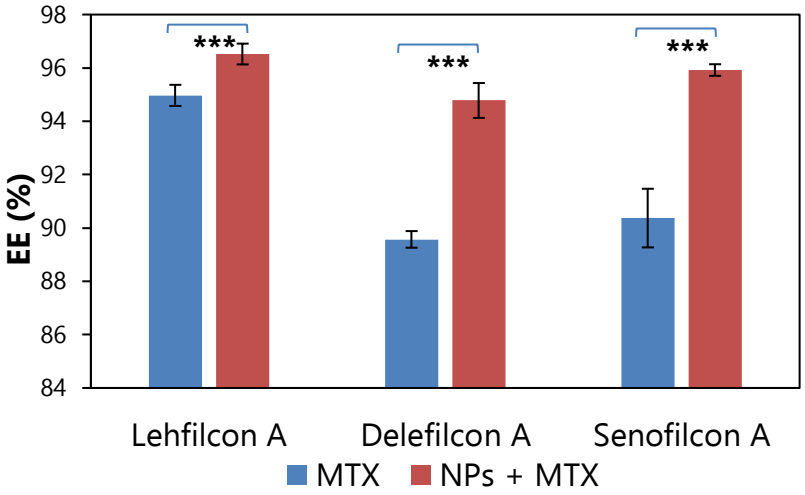


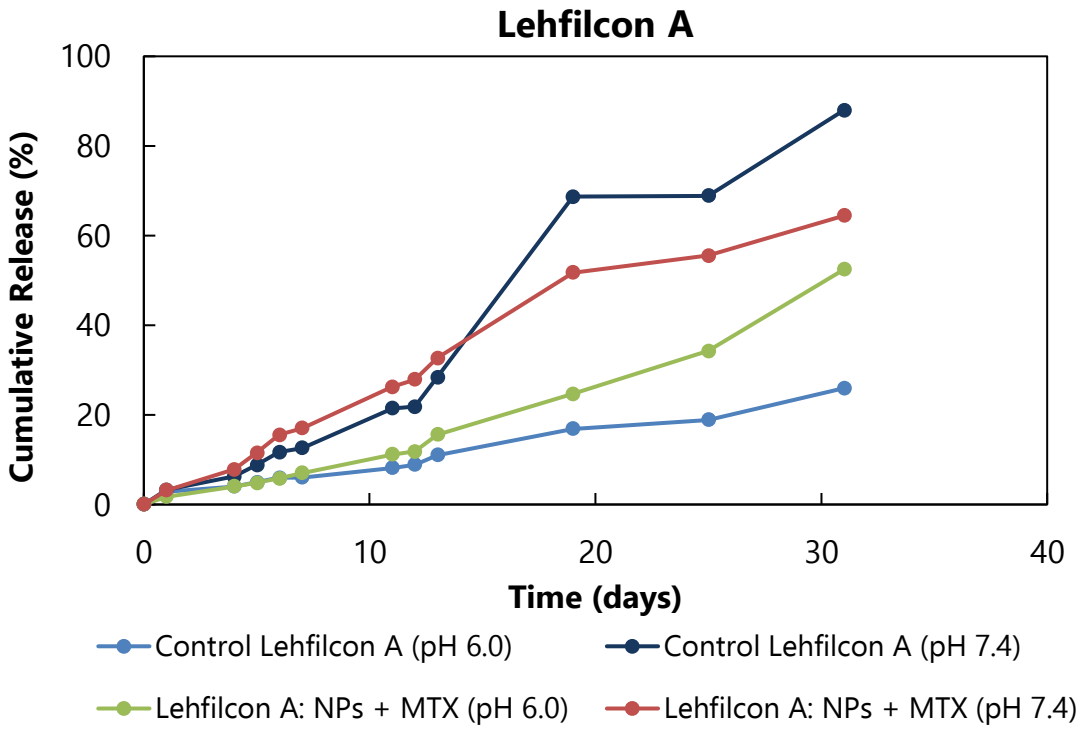
Figure 13. Encapsulation efficiency of MTX in CLs. Error bars correspond to standard deviation. “ns” means non-significant ($p > 0.05$), “*” means $p \leq 0.05$, “**” means $p \leq 0.01$, “***” means $p \leq 0.001$.

Regarding the Lehfilcon A CLs, the EE% with MTX alone has the value of 95 ± 0.4%, and with the previously encapsulated MTX (NPs + MTX), it presents an EE% of 97 ± 0.4%, indicating

a statistically significant difference ($p < 0.001$). This difference is also found between the two methods in the other two types of CLs. The Delefilcon A CLs present an EE% of MTX alone of 90 ± 0.3%, and with NPs + MTX, the EE% corresponds to 95 ± 0.7%. Analyzing the Senofilcon A CLs, the EE% of MTX alone resulted in 90 ± 1%, while with the encapsulation of the drug in NPs, the EE% increased to 96 ± 0.2%. It is concluded that the data reveals a relevant improvement in the encapsulation efficiency (EE%) of MTX in CLs when transported by Ch/HA NPs. This represents a considerable optimization in the incorporation of MTX into CLs, and this increase potentially translates into greater ocular bioavailability.

4.6 Drug release tests on contact lenses

The release profiles of MTX by the three types of CLs were evaluated with and without encapsulation in NPs and under two pH conditions, 6.0 and 7.4.



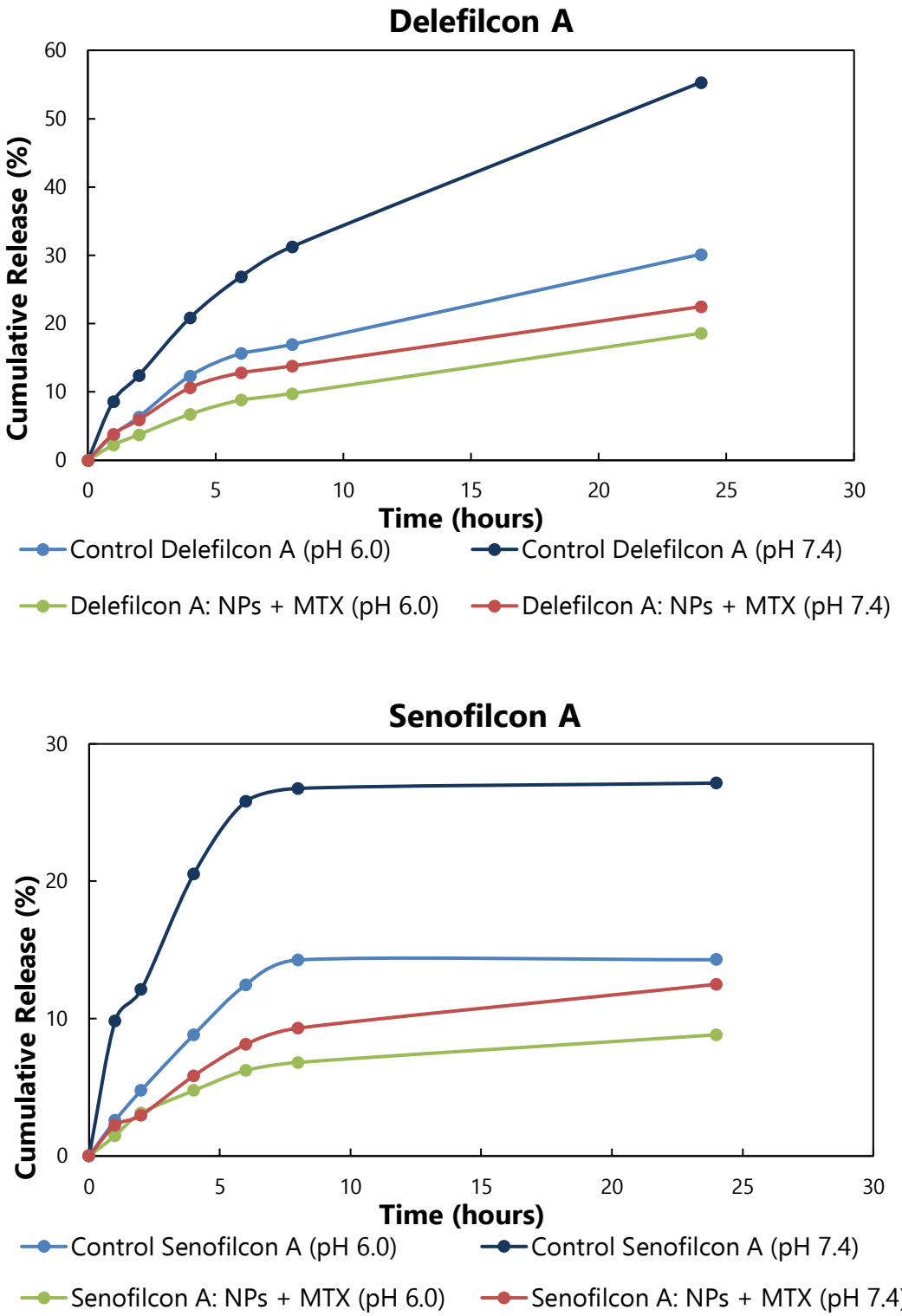


Figure 14. Plot of the release of MTX by the three types of contact lenses in pH 6.0 and pH 7.4. Control = CL with MTX adsorption only.

For monthly CLs, Lehfilcon A, MTX release was monitored over 32 days. **Figure 14** shows a significantly higher release in the control samples (without NPs) for pH 7.4, reaching

88 ± 18% at the end of the period. The formulation containing NPs + MTX at pH 7.4 also showed a marked release (64 ± 4%), but in a more controlled and progressive manner. At pH 6.0, both the control formulation (26 ± 2%) and the one with nanoparticles (53% ± 1) showed a reduced release compared to the CLs at pH 7.4. These results indicate that physiological pH favors drug diffusion, while the presence of nanoparticles promotes sustained release over time.

In the case of daily CLs, the study was carried out over 24 hours. Analyzing **Figure 15**, Delefilcon A, a rapid release is observed in the first hours, particularly in the control formulation at pH 7.4, which reached 55 ± 3% of drug released. The formulations with NPs presented lower release profiles, with 22 ± 2% of cumulative release of drug content at ph 7.4 and 19 ± 0.6% at pH 6.0. NPs were able to significantly reduce and control drug release, which is desirable for prolonged administration. This behavior reinforces the role of NPs in modulating release and highlights the impact of pH on increasing drug diffusion. The release profile of this lens is faster compared to the first day release of the Lehfilcon A lens.

The third lens in the study, Senofilcon A, had the most controlled and stable profile among the materials analyzed, with all groups remaining below 30% over 24 hours. The control formulation at pH 7.4 exhibited the highest value (27 ± 10%), stabilizing rapidly after 8 hours.Similar to the other CLs, formulations containing NPs showed the lowest release percentages, with 13 ± 3% at pH 7.4 and 9 ± 0.8% at pH 6.0, with sustained and progressive profiles. These results indicate that Senofilcon A is the most effective material for controlled release of MTX, with a lower risk of concentration peaks. This may be due to various factors related to the physicochemical properties of the material. Senofilcon A has the lowest water content compared to the other CLs in this study, which implies lower molecular mobility, reducing the drug diffusion rate to the external medium. This material may also have a higher affinity for MTX through hydrophobic interactions or hydrogen bonds, favouring the retention of the drug within the lens matrix.

It can be concluded that the presence of NPs has a significant effect on reducing and controlling the release rate, promoting more sustained profiles. This improvement may occur due to a more uniform drug distribution within the CLs matrix and better control over the drug

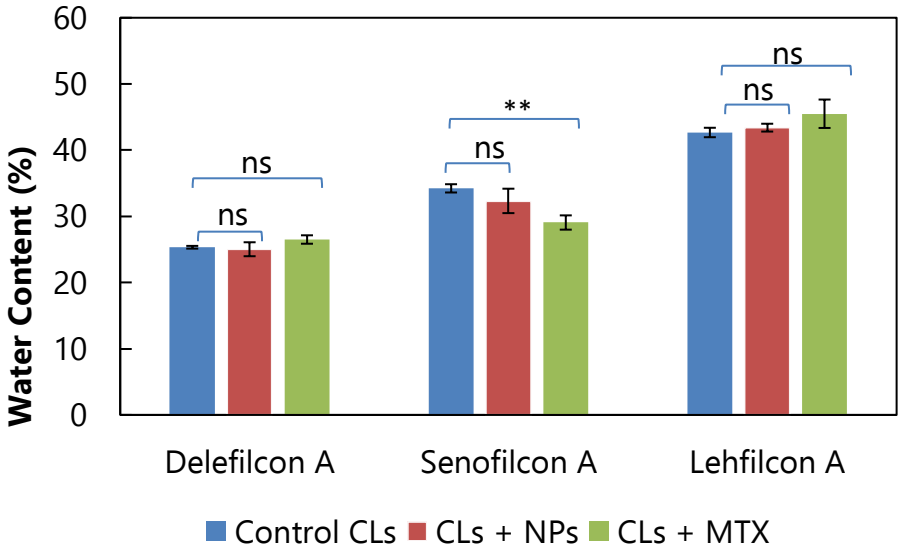
loading in the system. The release rate was shown to be lower at pH 6.0, which shows that this system is highly sensitive to pH alterations.

It can also be admitted that the Lehfilcon A lens is the one that allows greater release over days, suggesting an application in long-term therapies, while Delefilcon A and Senofilcon A are more indicated for release in hours, with Senofilcon A being the material with the greatest controlled drug release profile.

4.7 Characterization of contact lenses

4.7.1 Refractive index and water content

In this study, the RI and WC of the three CLs materials were evaluated under three conditions: new lens from the blister without any additive (control), lens with incorporation of NPs without MTX (CLs + NPs), and lens with incorporation of MTX (CLs + MTX), and the results are shown in **Figure 15**.



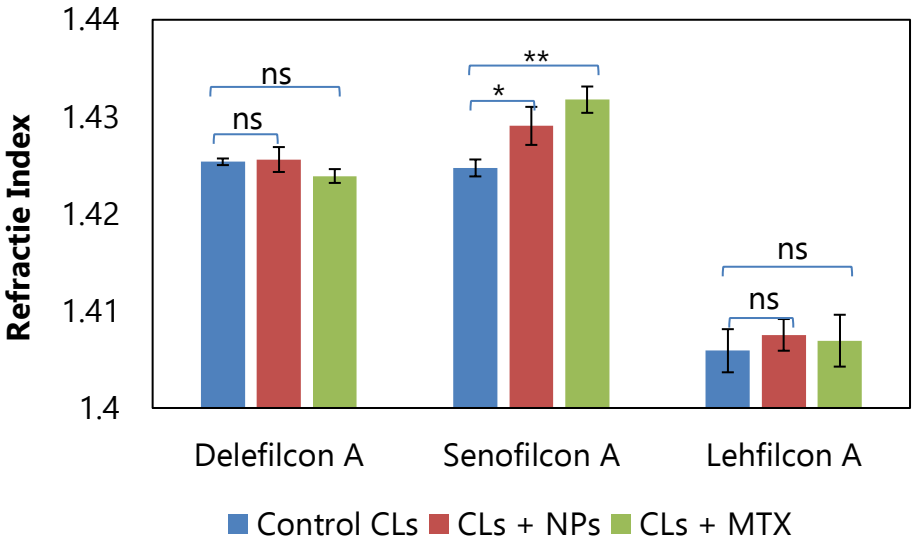


Figure 15. Refractive index and water content of CLs. Control = CL that was not immersed in any solution. Error bars correspond to standard deviation. "ns" means non-significant ($p > 0.05$), "*" means $p \leq 0.05$, "**" means $p \leq 0.01$, and "***" means $p \leq 0.001$.

Regarding RI and WC, the Delefilcon A lens does not undergo significant changes ($p > 0.05$) compared to the new lens in both conditions. The new lens had an RI of 1.4254 ± 0.0003, the NP-loaded lens had an RI of 1.4256 ± 0.0013, and the MTX-loaded lens had an RI of 1.4239 ± 0.0007. For WC, the new lens recorded an average value of 25.3 ± 0.21%; with incorporation of NPs, 25 ± 1.05%; and with incorporation of MTX, it recorded an average value of 26.5 ± 0.64%.

Unlike the previous one, the Senofilcon A lens showed significant differences for RI between the new lens and the two conditions. The new lens presented a value of 1.4247 ± 0.0009, and the CLs + NPs lens a value of 1.4291 ± 0.0020 ($p \leq 0.05$). The CLs + MTX condition recorded a mean value of 1.4318 ± 0.0014 and a p-value of $p \leq 0.01$. For WC, the CLs + MTX condition showed statistically significant differences in relation to the control ($p \leq 0.01$) with a value of 34.2 ± 0.62% for the control and 29.1 ± 1.08% with the incorporation of MTX. The only condition where no statistically significant differences were recorded was in the with incorporation of NPs, with a value of 32.3 ± 1.84%.

The monthly lens in this study, Lehfilcon A, showed no statistically significant differences ($p > 0.05$) in WC and RI after incorporation of NPs and MTX. Regarding RI, it

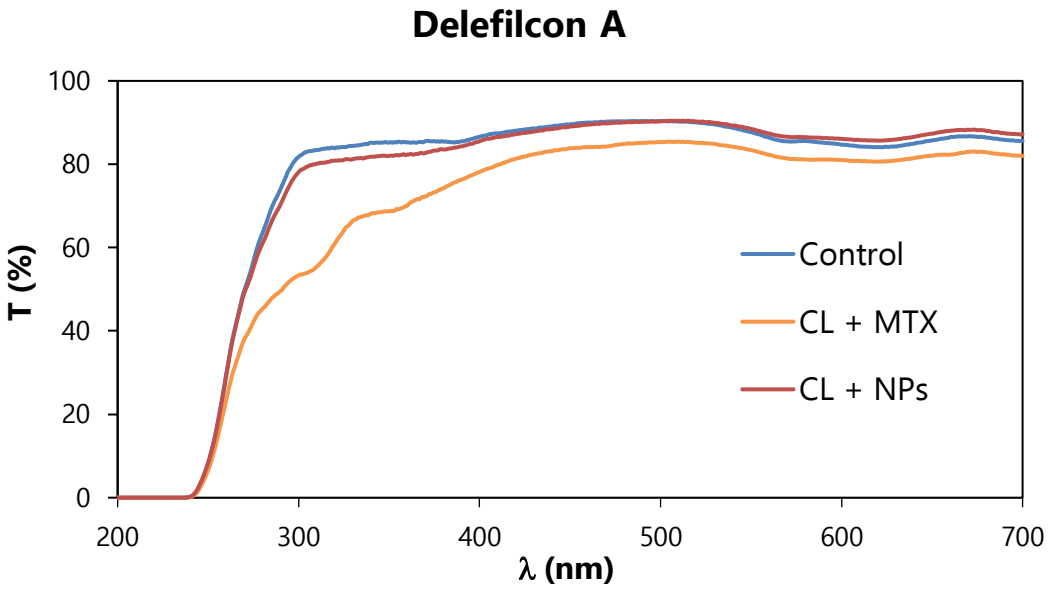
recorded an average value of 1.4059 ± 0.0022 for the control lens, 1.4075 ± 0.0016 for CLs + NPs, and 1.4069 ± 0.0027 for CLs + MTX. Regarding WC, it was measured an average of 42.7 ± 0.71% for the control lens, 43.4 ± 0.59% for CLs + NPs, and 45.5 ± 2.14% for CLs + MTX.

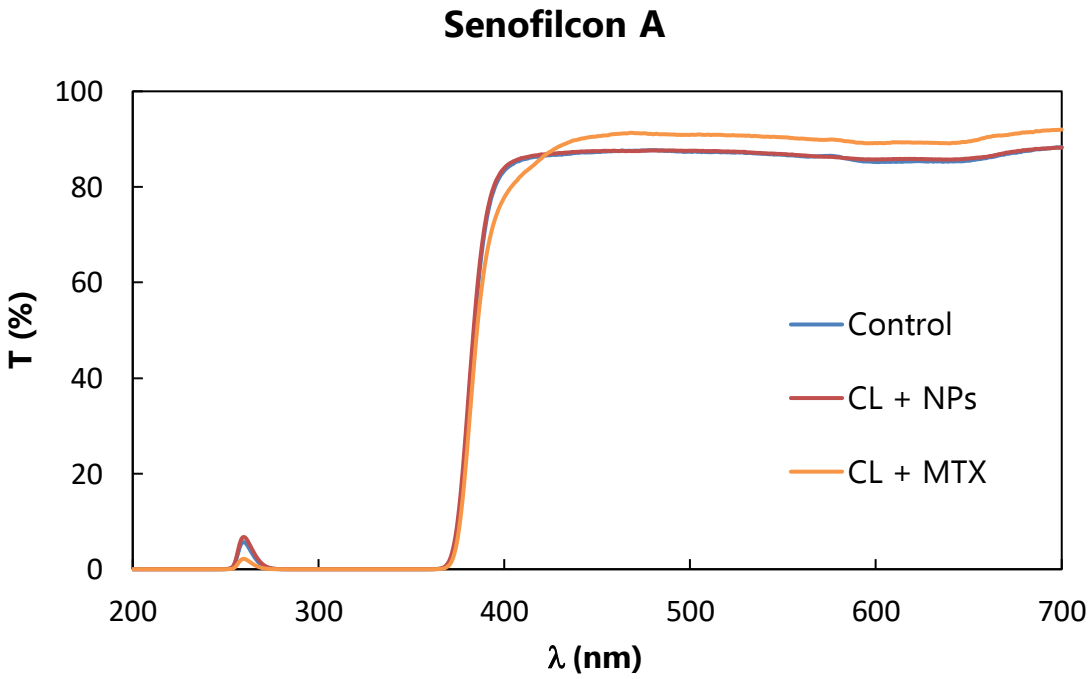
The results demonstrate that the incorporation of Ch/HA and MTX nanoparticles did not alter the water content (WC) or the refractive index (RI) of the Delefilcon A and Lehfilcon A lenses, suggesting that these materials possess a higher stability or resilience to surface modifications. This stability may be related to their surface treatments and material formulations, which are specifically designed to maintain lens properties even under exposure to external agents. In contrast, the Senofilcon A daily lens exhibited changes in RI following nanoparticle incorporation. This could indicate a greater susceptibility of this material to surface interactions, possibly due to differences in its bulk composition, surface chemistry, or water gradient technologies compared to Delefilcon A and Lehfilcon A.

These findings highlight the importance of material selection when designing nanoparticle-coated contact lenses, especially for drug delivery purposes, where maintaining the original optical and hydration properties of the lens is critical for user comfort and visual performance.

4.7.2 Transmittance

Through **Figure 16** it is possible to observe the transmittance of the three CLs in the UV-visible region and in three different conditions: new lens from the blister without any additive (control), lens with incorporation of NPs without MTX (CLs + NPs), and lens with incorporation of MTX (CLs + MTX).


Delefilcon A
100
80
60
40
20
0
T (%)
200
300
400
500
600
700
λ (nm)
Control
CL + MTX
CL + NPs


Senofilcon A
100
80
60
40
20
0
T (%)
200
300
400
500
600
700
λ (nm)
Control
CL + NPs
CL + MTX

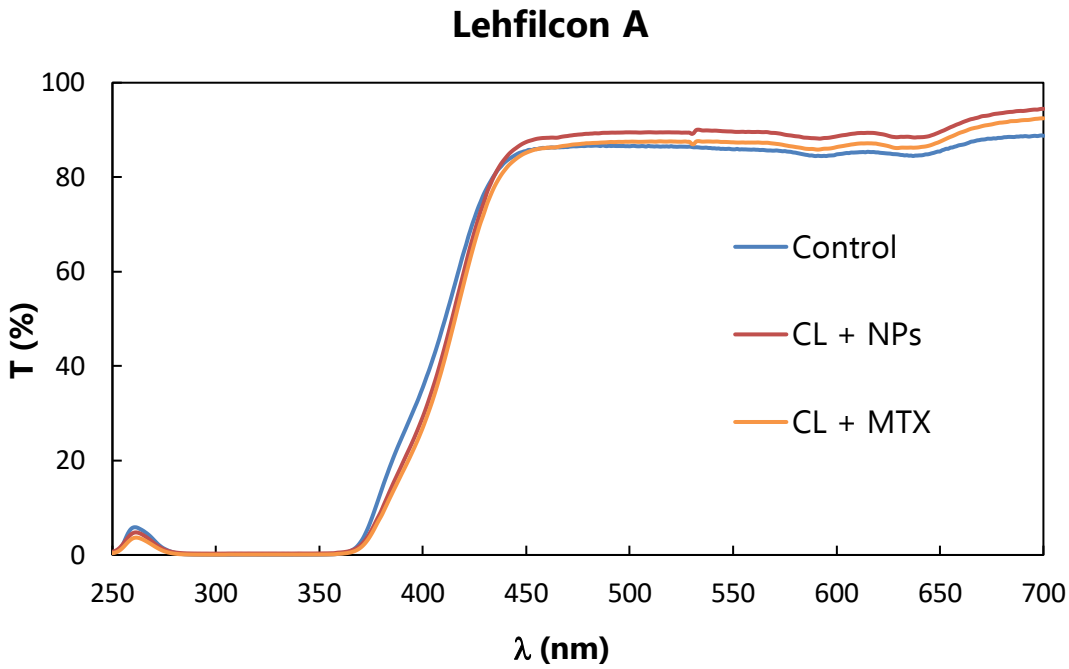


Figure 16. Transmittance spectra of CLs. Control = CL that were not immersed in any solution.

The Delefilcon A lens demonstrated the greatest sensitivity to modifications. The new lens maintained high optical transparency, with transmittance above 85% at wavelengths from 350 to 700 nm. The presence of NPs slightly reduced the transmittance below 400 nm but maintained a value above 85% between 400 and 700 nm. However, the addition of MTX resulted in a drop in transmittance compared to the two previous conditions, being more noticeable before 400 nm, and above this wavelength it varied between 80% and 85% of T (%).

Unlike Delefilcon A lens material, Senofilcon A lens contains a class I UV filter (protects against UV-A (96%) and UV-B (99.9%) radiation)[44], and, therefore, values of 0% are observed for wavelengths below 400 nm. The three conditions tested showed similar behavior: transmittance above 85% from 400 nm to 700nm. A slight increase in the transmittance of samples containing MTX was even observed compared to the others, which may suggest a slight improvement in transparency induced by the chemical modification of the lens.

The monthly replacement CLs, Lehfilcon A, also have 0% transmittance values below 400 nm but, in addition to the class I UV filter (protects against UV-A (90%) and UV-B (99%)

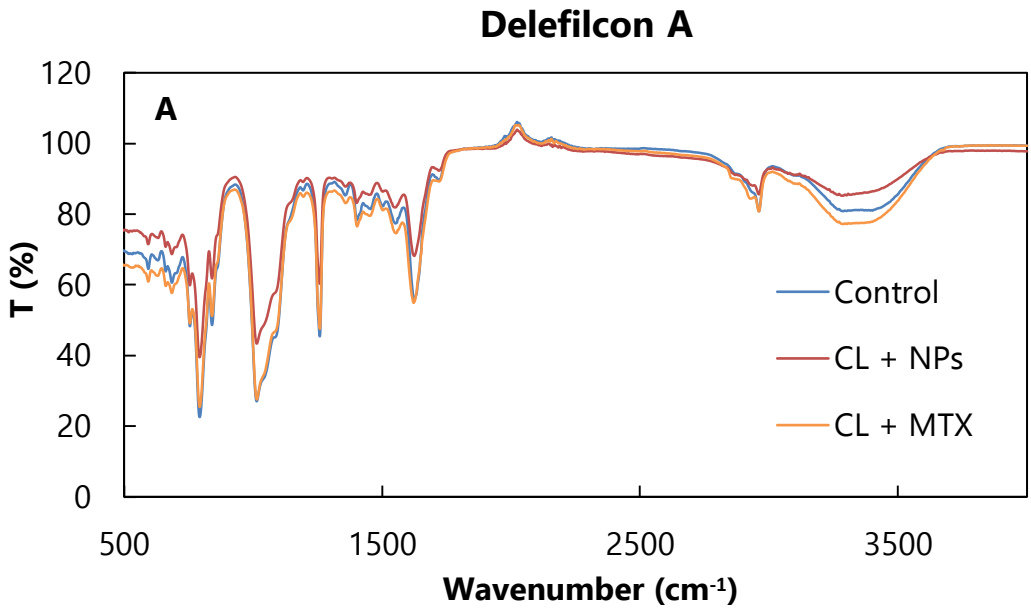
radiation), also filters high-energy visible light (HEVL) that enters the eye (34%) in the region of wavelengths between 380 and 450 nm.[42] Similarly to Senofilcon A lenses, all conditions recorded transmittance greater than 85% after 400 nm. There was a small positive difference in the curve of the CLs + NPs condition, which showed a slight improvement in transmittance compared to the control.

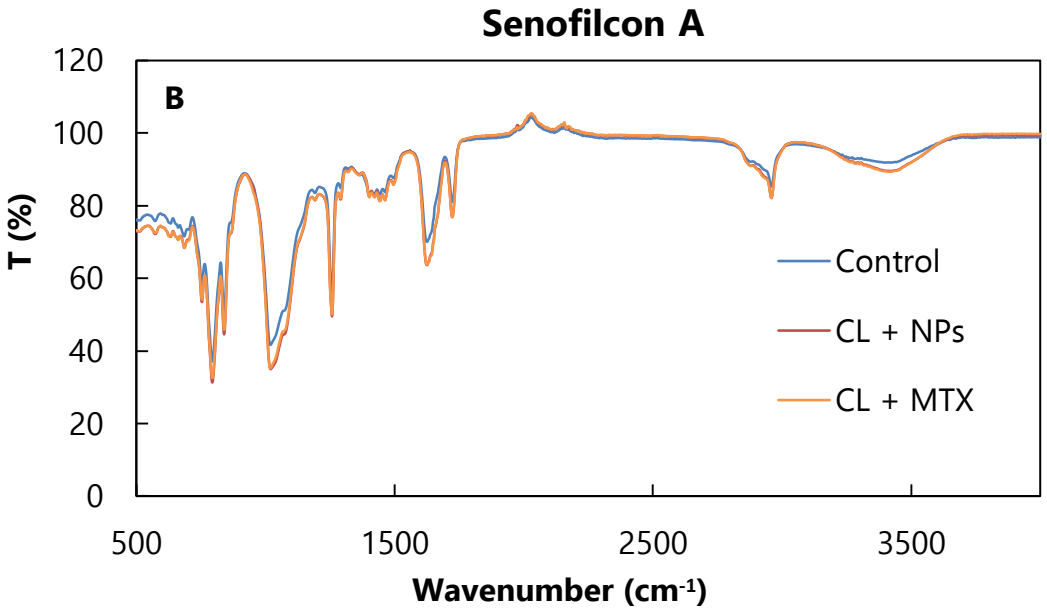
It is concluded that among the three materials tested, Delefilcon A was the only lens whose transparency was affected by the incorporation of MTX. In contrast, both Senofilcon A and Lehfilcon A maintained their optical clarity following the addition of either nanoparticles or MTX.

The reduction in transparency observed in Delefilcon A could be attributed to specific interactions between the material's unique surface characteristics and the incorporated MTX molecules, potentially leading to aggregation or changes in surface homogeneity. Given that Delefilcon A employs a water gradient technology with a high surface water content, it is possible that the introduction of hydrophobic or poorly dispersed drug molecules disrupted the surface organization, resulting in increased light scattering. Meanwhile, the stable transparency of Senofilcon A and Lehfilcon A suggests that their material matrices are more capable of integrating nanoparticles and drug molecules without compromising the optical properties. These results underscore the importance of considering material composition, surface structure, and water content when designing drug-eluting contact lenses to ensure the preservation of critical properties such as transparency.

4.7.3 Fourier transform infrared spectroscopy

FTIR analysis allowed the identification of chemical differences between new CLs (control) and CLs with the addition of NPs and MTX. It allowed us to verify interactions between the polymers and the drug and confirm the presence of each component in the CLs.


Delefilcon A
A
120
100
80
60
40
20
0
T (%)
500
1500
2500
3500
Wavenumber (cm-1)
Control
CL + NPs
CL + MTX


Senofilcon A
B
120
100
80
60
40
20
0
T (%)
500
1500
2500
3500
Wavenumber (cm-1)
Control
CL + NPs
CL + MTX

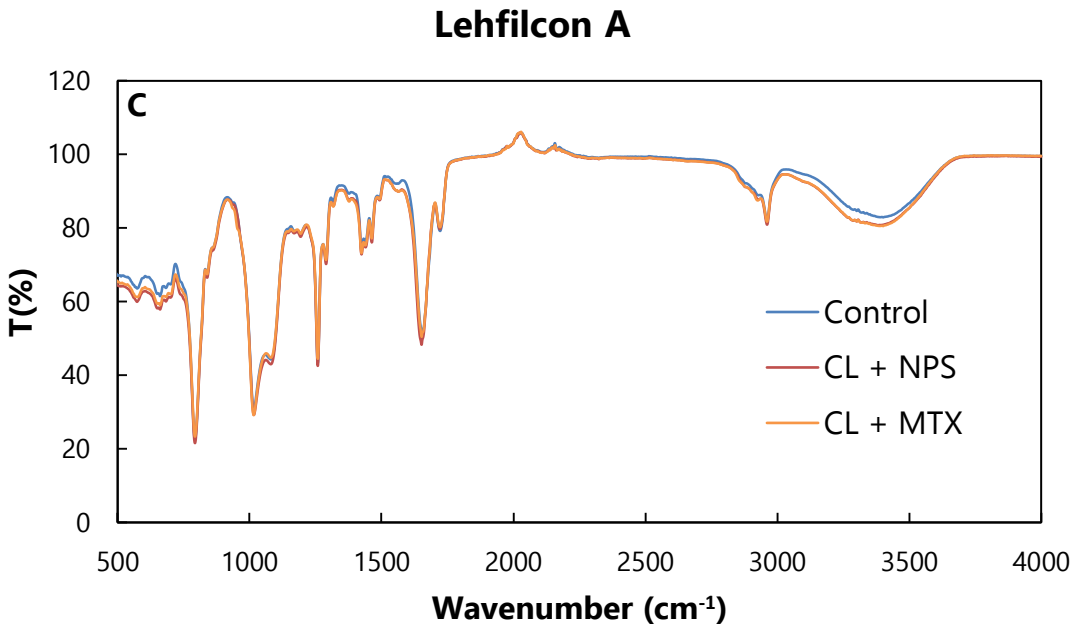


Figure 17. Infrared spectrum of the three types of CLs in 3 conditions: CLs with Ch/HA nanoparticles, CLs with MTX, and CLs that were not immersed in any solution (Control). Delefilcon A CLs (**A**); Senofilcon A (**B**); Lehfilcon A (**C**).

FTIR graph analysis of CLs Delefilcon A (**Figure 17 A**) showed spectral changes between the samples containing NPs and MTX and the control. The stretching vibrations of the C=O (carbonyl) and C=C (aromatic) groups in the MTX structure, which are responsible for the MTX-loaded sample's more intense band around 1650 cm^{-1}, confirmed the MTX's integration into the lens matrix.[61] In addition, the sample with nanoparticles showed an increase in absorbance in the 1000–1100 cm^{-1} area, which was probably caused by the presence of P=O and C–O vibrations from tripolyphosphate (TPP) or other phosphate-containing groups.[60]

The O–H/N–H stretching band around 3300 cm^{-1} was also shown to be wider and more intense in both modified samples, indicating the presence of hydrogen bonding or other intermolecular interactions between the additives (chitosan, HA, and MTX) and the lens's polymeric structure. Characteristic peaks of CLs, such as the broad O–H/N–H stretching band around 3300 cm^{-1}, the aliphatic C–H stretching near 2900 cm^{-1}, the amide I band (1650 cm^{-1}) and amide II band (1580 cm^{-1}), as well as the Si–O–Si or C–O stretching region (1000–1100 cm^{-1}), are consistently present across all samples. This indicates that incorporation of

nanoparticles and MTX does not disrupt the core polymeric structure of Delefilcon A but induces localized chemical interactions.

For Senofilcon A CLs (**Figure 17 B**), in the spectrum of the control lens (unmodified), bands characteristic of the Senofilcon A polymer matrix are observed, namely, the Si–O–Si stretching band in the region of 1000–1100 cm^{-1}, associated with the presence of siloxane groups, as well as bands in the region of 2800–3000 cm^{-1}, attributed to the C–H stretching of aliphatic chains.

Modified lenses (CLs + NPs and CLs + MTX) showed consistent but minor alterations in many spectral regions, indicating the presence of functional groups typical of the added compounds. The presence of P=O groups from TPP, as well as C–O and C–N from hyaluronic acid and chitosan, may be the cause of the minor increase in peak intensity seen in the 1000–1150 cm^{-1} region.

The region between 1550 and 1650 cm^{-1} showed intensification of the peaks in the modified lenses, indicating the presence of Amide I (C=O) and Amide II (N–H) bands, explained by chitosan peptide bonds and the amide group present in the MTX structure. In addition, a decrease in transmittance was noted in the CLs + NPs and CLs + MTX samples in the 3200–3500 cm^{-1} range. This was caused by an increase in hydroxyl (–OH) and amine (–NH) groups, which are traits of both the drug and natural polymers. Despite the observed changes, the overlap of the main peaks of the control lens with the other two conditions proves that the main structure of the Senofilcon A lens remained stable during the incorporation process. The slight differences in peaks in key regions confirm the presence of the incorporated compounds (NPs and MTX).

FTIR spectra of Lehfilcon A (**Figure 17 C**) CLs under control, nanoparticle-loaded, and MTX-loaded conditions reveal higher similarity, particularly in the main characteristic peaks of the CLs material. The absorption bands, including those around 3300 cm^{-1} (O–H/N–H stretching), 2900 cm^{-1} (C–H stretching), 1650 cm^{-1} (C=O stretching, Amide I), and 1000–1100 cm^{-1} (Si–O–Si or C–O stretching), appear in all three conditions. Minor variations in peak intensity and shape are observed, especially in the 1650 cm^{-1} and 3300 cm^{-1} regions for the MTX and NP-loaded lenses, which may indicate intermolecular interactions with the additives. However, no significant shifts or disappearance of major peaks are observed, indicating that

the polymeric structure of Lehfilcon A remains chemically stable and is not disrupted by the incorporation of nanoparticles or methotrexate.

5. CONCLUSIONS AND FUTURE WORK

5.1 Conclusions

According to the results obtained in this work can be concluded:

- The solutions with a higher concentration of chitosan show the presence of aggregates.
- Ch/HA NPs solutions must be stored at a temperature of 4°C to maintain their characteristics, such as size and homogeneity.
- The optimal concentrations for the synthesis of Ch/HA NPs with the method of ionotropic gelation are 0.0025 wt% TPP, 0.0050 wt% Ch, and 0.05 wt% HA.
- The Ch/HA NPs presented a hydrodynamic diameter of 286 ± 14 nm, polydispersity of 0.13 ± 0.04, and a zeta potential of -11.13 ± 0.40 mV when measured by DLS, in a buffer solution (10 mM) of pH 7.4. These NPs maintained stability for at least 30 days.
- When Ch/HA NPs are measured by DLS, in a buffer solution (10 mM) of pH 6.0, they present a hydrodynamic diameter of 153 ± 7 nm, polydispersity of 0.08 ± 0.04, and a zeta potential of -16.98 ± 0.69 mV. The choice of a slightly more acidic pH is advantageous for preserving the stability of the NPs and lowering their propensity to aggregate.
- Analysis of SEM and STEM images revealed that the nanoparticles exhibit a spherical shape, average diameters of 130 ± 52 nm, and moderate polydispersity.
- The optimal concentration of MTX tested in this study is 500 µM. After encapsulation of MTX in Ch/HA NPs, there were no significant changes in size, polydispersity, and surface charge of the NPs.
- The FTIR spectrum of MTX-loaded Ch/HA nanoparticles demonstrates that each element was successfully incorporated into the nanoparticle system without exhibiting detectable chemical deterioration.
- MTX showed a good encapsulation efficiency in NPs of 97 ± 1.34 % and a drug loading capacity in NPs of 60 ± 4.49 %.
- The three types of CLs present in the study evidenced good NP adsorption efficiency. The daily replacement lenses, Delefilcon A and Senofilcon A presented values of 95 ± 0.6% (corresponding to 18.64 ± 0.1 mg of NPs) and 96% ± 0.6% (corresponding to 18.87

± 0.1 mg of NPs), respectively. The monthly replacement lens recorded a value of 96 ± 1%, corresponding to an NPs mass of 18.91 ± 0.2 mg.

- The encapsulation efficiency of MTX in CLs when it was encapsulated in NPs showed a relevant increase compared to the results of the isolated drug (EE% of 97 ± 0.4 % for Lehfilcon A, 95 ± 0.7 % for Delefilcon A, and 96 ± 0.2% for Senofilcon A), therefore concluding that Ch/HA NPs increase the bioavailability of the drug in the contact lenses present in the study.
- The presence of nanoparticles (NPs) has a significant effect on reducing and controlling the release rate, promoting more sustained profiles. After 24 hours, Delefilcon A and Senofilcon A released cumulatively 22 % and 13% of MTX, respectively, and Lehfilcon A released cumulatively 64% after 30 days, showing sustained release profiles. The null hypothesis (H0) of hypothesis 3 "Different CLs materials have significant differences in the incorporation and release profile of MTX." cannot be rejected.
- The incorporation of Ch/HA NPs and MTX did not alter the RI and WC of Lehfilcon A and Delefilcon A CLs, while Senofilcon A CLs showed significant changes ($p \leq 0.01$) in RI with the NPs and MTX, and for the WC, it only revealed changes with MTX. Therefore, the null hypothesis (H0) of hypothesis 2 " Ch/HA NPs with MTX cause significant changes in CLs properties." cannot be completely rejected
- No variations were found in the UV/visible transmittance of Lehfilcon A and Senofilcon A CLs after the incorporation of NPs and MTX, with %T always above 85% in the visible region. The Delefilcon A lens presented a lower transmittance value between 80% and 85% after incorporation of MTX, but with NPs, it recorded transmittance above 85%.
- In the analysis of FTIR measurements, no changes were found in the chemical structure of daily and monthly replacement CLs after immersion in the Ch/HA NPs solution and the MTX solution.
- Ch/HA NPs are suitable for sustained release of MTX from Lehfilcon A and Delefilcon A contact lenses, therefore, the null hypothesis (H0) of hypothesis 1 "The CLs selected for the study aren’t suitable for incorporating and releasing Ch/HA NPs with MTX. " can be rejected.
- Senofilcon A is a less suitable material for MTX delivery via Ch/HA NPs.

- The results obtained allow us to reject the null hypothesis (H0) of hypothesis 4 and accept the alternative hypothesis (H1): "The system of CLs+ NPs of Ch/HA with MTX is promising for a future ocular DDS.”.

5.2 Future work

Considering the promising results of this work, it would be relevant to study the following topics in the future:

- Measurement of oxygen permeability of contact lenses previously loaded with Ch/HA nanoparticles.
- Determine the modulus of elasticity and other mechanical properties of CLs containing Ch/HA NPs.
- Improving the stability of NPs using controlled flow at the reagent addition.
- Carrying out nanoparticle cytotoxicity tests.
- Assessment of the characteristics of CLs containing MTX-loaded Ch/HA NPs in interaction with CLs cleaning solutions.

6. REFERENCES

1. Jumelle, C., Gholizadeh, S., Annabi, N., & Dana, R. (2020). Advances and limitations of drug delivery systems formulated as eye drops. *Journal of Controlled Release*, *321*, 1–22. https://doi.org/10.1016/j.jconrel.2020.01.057

2. Rykowska, I., Nowak, I., & Nowak, R. (2021). Soft Contact Lenses as Drug Delivery Systems: A Review. *Molecules*, *26*(18), Article 18. https://doi.org/10.3390/molecules26185577

3. Rodrigues, F. S. C., Campos, A., Martins, J., Ambrósio, A. F., & Campos, E. J. (2020). Emerging Trends in Nanomedicine for Improving Ocular Drug Delivery: Light-Responsive Nanoparticles, Mesoporous Silica Nanoparticles, and Contact Lenses. *ACS Biomaterials Science & Engineering*, *6*(12), 6587–6597. https://doi.org/10.1021/acsbiomaterials.0c01347

4. *A comprehensive review of intravitreal immunosuppressants and biologicals used in ophthalmology*. (n.d.). https://doi.org/10.1177/25158414221097418

5. Wang, G., & Peng, X. (2020). A Review of Clinical Applications and Side Effects of Methotrexate in Ophthalmology. *Journal of Ophthalmology*, *2020*, 1–11. https://doi.org/10.1155/2020/1537689

6. Akiyama, H., Takase, H., Kubo, F., Miki, T., Yamamoto, M., Tomita, M., Mochizuki, M., Miura, O., & Arai, A. (2016). High-dose methotrexate following intravitreal methotrexate administration in preventing central nervous system involvement of primary intraocular lymphoma. *Cancer Science*, *107*(10), 1458–1464. https://doi.org/10.1111/cas.13012

7. Abdi, F., Mohammadi, S. S., & Falavarjani, K. G. (2021). Intravitreal Methotrexate. *Journal of Ophthalmic & Vision Research*, *16*(4), 657–669. https://doi.org/10.18502/jovr.v16i4.9756

8. Gomes, J. A. P., Azar, D. T., Baudouin, C., Efron, N., Hirayama, M., Horwath-Winter, J., Kim, T., Mehta, J. S., Messmer, E. M., Pepose, J. S., Sangwan, V. S., Weiner, A. L., Wilson, S. E., & Wolffsohn, J. S. (2017). TFOS DEWS II iatrogenic report. *The Ocular Surface*, *15*(3), 511–538. https://doi.org/10.1016/j.jtos.2017.05.004

9. Valachová, K., Hassan, M. E., & Šoltés, L. (2024). Hyaluronan: Sources, Structure, Features and Applications. *Molecules*, *29*(3), 739. https://doi.org/10.3390/molecules29030739

10. Hynnekleiv, L., Magno, M., Vernhardsdottir, R. R., Moschowits, E., Tønseth, K. A., Dartt, D. A., Vehof, J., & Utheim, T. P. (2022). Hyaluronic acid in the treatment of dry eye disease. *Acta Ophthalmologica*, *100*(8), 844–860. https://doi.org/10.1111/aos.15159

11. Wang, T.-J., Rethi, L., Ku, M.-Y., Nguyen, H. T., & Chuang, A. E.-Y. (2024). A review on revolutionizing ophthalmic therapy: Unveiling the potential of chitosan, hyaluronic acid, cellulose, cyclodextrin, and poloxamer in eye disease treatments. *International Journal of Biological Macromolecules*, *273*, 132700. https://doi.org/10.1016/j.ijbiomac.2024.132700

12. Hashad, R. A., Ishak, R. A. H., Geneidi, A. S., & Mansour, S. (2017). Surface functionalization of methotrexate-loaded chitosan nanoparticles with hyaluronic acid/human serum albumin: Comparative characterization and in vitro cytotoxicity. *International Journal of Pharmaceutics*, *522*(1), 128–136. https://doi.org/10.1016/j.ijpharm.2017.03.008

13. Hashad, R. A., Ishak, R. A. H., Geneidi, A. S., & Mansour, S. (2016). Methotrexate loading in chitosan nanoparticles at a novel pH: Response surface modeling, optimization and characterization. *International Journal of Biological Macromolecules*, *91*, 630–639. https://doi.org/10.1016/j.ijbiomac.2016.06.014

14. Yermak, I. M., Davydova, V. N., & Volod'ko, A. V. (2022). Mucoadhesive Marine Polysaccharides. *Marine Drugs*, *20*(8), 522. https://doi.org/10.3390/md20080522

15. Ahmed, S., Amin, M. M., & Sayed, S. (2023). Ocular Drug Delivery: A Comprehensive Review. *AAPS PharmSciTech*, *24*(2), 66. https://doi.org/10.1208/s12249-023-02516-9

16. *CONTACT LENSES 2023*. (n.d.). PentaVision. Retrieved 5 October 2024, from https://clspectrum.com/issues/2024/januaryfebruary/contact-lenses-2023/

17. Zhang, X., Cao, X., & Qi, P. (2020). Therapeutic contact lenses for ophthalmic drug delivery: Major challenges. *Journal of Biomaterials Science. Polymer Edition*, *31*(4), 549–560. https://doi.org/10.1080/09205063.2020.1712175

18. Musgrave, C. S. A., & Fang, F. (2019). Contact Lens Materials: A Materials Science Perspective. *Materials*, *12*(2), Article 2. https://doi.org/10.3390/ma12020261

19. Yang, H., Zhao, M., Xing, D., Zhang, J., Fang, T., Zhang, F., Nie, Z., Liu, Y., Yang, L., Li, J., & Wang, D. (2023). Contact lens as an emerging platform for ophthalmic drug delivery: A systematic review. *Asian Journal of Pharmaceutical Sciences*, *18*(5), 100847. https://doi.org/10.1016/j.ajps.2023.100847

20. Yang, M., Yang ,Yangfan, Lei ,Ming, Ye ,Chengtian, Zhao ,Chunshun, Xu ,Jiangang, Wu ,Kaili, & and Yu, M. (2016). Experimental studies on soft contact lenses for controlled ocular delivery of pirfinedone: In vitro and in vivo. *Drug Delivery*, *23*(9), 3538–3543. https://doi.org/10.1080/10717544.2016.1204570

21. Phan, C.-M., Subbaraman, L. N., & Jones, L. (2013). In Vitro Uptake and Release of Natamycin From Conventional and Silicone Hydrogel Contact Lens Materials. *Eye & Contact Lens*, *39*(2), 162. https://doi.org/10.1097/ICL.0b013e31827a7a07

22. Hui, A. (2017). Contact lenses for ophthalmic drug delivery. *Clinical and Experimental Optometry*, *100*(5), 494–512. https://doi.org/10.1111/cxo.12592

23. Soluri, A., Hui, A., & Jones, L. (2012). Delivery of Ketotifen Fumarate by Commercial Contact Lens Materials. *Optometry and Vision Science*, *89*(8), 1140. https://doi.org/10.1097/OPX.0b013e3182639dc8

24. Maulvi, F. A., Desai, D. T., Shetty, K. H., Shah, D. O., & Willcox, M. D. P. (2021). Advances and challenges in the nanoparticles-laden contact lenses for ocular drug delivery.

International Journal of Pharmaceutics, *608*, 121090. https://doi.org/10.1016/j.ijpharm.2021.121090

25. Chen, Q., Wang, S., Liu, H., Ibrahim, S., Oladejo, A. O., Man, J., Hao, B., & Yang, Z. (2024). Novel Drug Delivery Systems: An Important Direction for Drug Innovation Research and Development. *Pharmaceutics*, *16*. https://doi.org/10.3390/pharmaceutics16050674

26. Sivadasan, D., Sultan, M. H., Madkhali, O., Almoshari, Y., & Thangavel, N. (2021). Polymeric Lipid Hybrid Nanoparticles (PLNs) as Emerging Drug Delivery Platform—A Comprehensive Review of Their Properties, Preparation Methods, and Therapeutic Applications. *Pharmaceutics*, *13*(8), 1291. https://doi.org/10.3390/pharmaceutics13081291

27. Jafernik, K., Ładniak, A., Blicharska, E., Czarnek, K., Ekiert, H., Wiącek, A. E., & Szopa, A. (2023). Chitosan-Based Nanoparticles as Effective Drug Delivery Systems—A review. *Molecules*, *28*(4), Article 4. https://doi.org/10.3390/molecules28041963

28. Nasr, F. H., Khoee, S., Dehghan, M. M., Chaleshtori, S. S., & Shafiee, A. (2016). Preparation and Evaluation of Contact Lenses Embedded with Polycaprolactone-Based Nanoparticles for Ocular Drug Delivery. *Biomacromolecules*, *17*(2), 485–495. https://doi.org/10.1021/acs.biomac.5b01387

29. Janagam, D. R., Lowe, T. L., & Wu, L. (2017). Nanoparticles for drug delivery to the anterior segment of the eye. *Advanced Drug Delivery Reviews*, *122*. https://doi.org/10.1016/j.addr.2017.04.001

30. Thanou, M., Verhoef, J. C., & Junginger, H. E. (2001). Chitosan and its derivatives as intestinal absorption enhancers. *Advanced Drug Delivery Reviews*, *50*, S91–S101. https://doi.org/10.1016/S0169-409X(01)00180-6

31. Nasti, A., Zaki, N. M., de Leonardis, P., Ungphaiboon, S., Sansongsak, P., Rimoli, M. G., & Tirelli, N. (2009). Chitosan/TPP and Chitosan/TPP-hyaluronic Acid Nanoparticles: Systematic Optimisation of the Preparative Process and Preliminary Biological Evaluation. *Pharmaceutical Research*, *26*(8), 1918–1930. https://doi.org/10.1007/s11095-009-9908-0

32. Yilmaz Atay, H. (2019). Antibacterial Activity of Chitosan-Based Systems. In S. Jana & S. Jana (Eds.), *Functional Chitosan: Drug Delivery and Biomedical Applications* (pp. 457–489). Springer. https://doi.org/10.1007/978-981-15-0263-7_15

33. Vigani, B., Rossi, S., Sandri, G., Bonferoni, M. C., Caramella, C. M., & Ferrari, F. (2019). Hyaluronic acid and chitosan-based nanosystems: A new dressing generation for wound care. *Expert Opinion on Drug Delivery*, *16*(7), 715–740. https://doi.org/10.1080/17425247.2019.1634051

34. Myint, S. S., Laomeephol, C., Thamnium, S., Chamni, S., & Luckanagul, J. A. (2023). Hyaluronic Acid Nanogels: A Promising Platform for Therapeutic and Theranostic

Applications. *Pharmaceutics*, *15*(12), 2671. https://doi.org/10.3390/pharmaceutics15122671

35. Hoang, N. H., Le Thanh, T., Sangpueak, R., Treekoon, J., Saengchan, C., Thepbandit, W., Papathoti, N. K., Kamkaew, A., & Buensanteai, N. (2022). Chitosan Nanoparticles-Based Ionic Gelation Method: A Promising Candidate for Plant Disease Management. *Polymers*, *14*(4), 662. https://doi.org/10.3390/polym14040662

36. Maksimovic, V., Pavlovic-Popovic, Z., Vukmirovic, S., Cvejic, J., Mooranian, A., Al-Salami, H., Mikov, M., & Golocorbin-Kon, S. (2020). Molecular mechanism of action and pharmacokinetic properties of methotrexate. *Molecular Biology Reports*, *47*(6), 4699–4708. https://doi.org/10.1007/s11033-020-05481-9

37. Gu, J., Jiang, T., Liu, S., Chen, X., Wang, Z., Zhang, P., Wang, L., Jiang, R., Huang, X., Xu, G., & Chang, Q. (2023). Longitudinal Analysis of Ocular Manifestation and Interleukin During Intravitreal Treatment of Vitreoretinal Lymphoma With Methotrexate. *American Journal of Ophthalmology*, *251*, 189–196. https://doi.org/10.1016/j.ajo.2023.03.010

38. Frenkel, S., Hendler, K., Siegal, T., Shalom, E., & Pe'er, J. (2008). Intravitreal methotrexate for treating vitreoretinal lymphoma: 10 years of experience. *British Journal of Ophthalmology*, *92*(3), 383–388. https://doi.org/10.1136/bjo.2007.127928

39. Habot-Wilner, Z., Frenkel, S., & Pe'er, J. (2021). Efficacy and safety of intravitreal methotrexate for vitreo-retinal lymphoma – 20 years of experience. *British Journal of Haematology*, *194*(1), 92–100. https://doi.org/10.1111/bjh.17451

40. Jeong, Y., Ryu, J. S., Park, U. C., & Oh, J. Y. (2020). Corneal Epithelial Toxicity after Intravitreal Methotrexate Injection for Vitreoretinal Lymphoma: Clinical and In Vitro Studies. *Journal of Clinical Medicine*, *9*(8), 2672. https://doi.org/10.3390/jcm9082672

41. Lira, M., Pereira, C., Real Oliveira, M. E. C. D., & Castanheira, E. M. S. (2015). *Importance of contact lens power and thickness in oxygen transmissibility*. https://doi.org/10.1016/j.clae.2014.12.002

42. Mathew, J. (2023). *TOTAL30® CONTACT LENSES WITH WATER GRADIENT AND CELLIGENT® TECHNOLOGIES* [White Paper]. https://alcon.widen.net/s/rz98bfrbsh/us---total30-contact-lenses-with-water-gradient-and-celligent-technologies

43. Mathew, J. (2022). *DAILIES TOTAL1® CONTACT LENSES WITH WATER GRADIENT AND SMARTEARS® TECHNOLOGY*. https://alcon.widen.net/s/6hjvfgq8xc/dt1dt1fa-white-paper

44. Johnson & Johnson. (2022). *ACUVUE® 2022 CATÁLOGO DE LENTES DE CONTACTO* [White Paper]. https://jnjvisionpro.com.ar/sites/ar/files/public/pdf/catalogo2022_arg_baja.pdf

45. Anton Paar. (n.d.). *Understanding the Concept of Dynamic Light Scattering* (p. 2017) [White Paper].

46. Cohen, S. M. (n.d.). *Modular Spectrofluorometer The Fluorolog®-3* [Feature Article].

47. Lin, P.-C., Lin, S., Wang, P. C., & Sridhar, R. (2014). Techniques for physicochemical characterization of nanomaterials. *Biotechnology Advances*, *32*(4), 711–726. https://doi.org/10.1016/j.biotechadv.2013.11.006

48. Inkson, B. J. (2016). 2—Scanning electron microscopy (SEM) and transmission electron microscopy (TEM) for materials characterization. In G. Hübschen, I. Altpeter, R. Tschuncky, & H.-G. Herrmann (Eds.), *Materials Characterization Using Nondestructive Evaluation (NDE) Methods* (pp. 17–43). Woodhead Publishing. https://doi.org/10.1016/B978-0-08-100040-3.00002-X

49. González-Méijome, J. M., Lira, M., López-Alemany, A., Almeida, J. B., Parafita, M. A., & Refojo, M. F. (2006). Refractive index and equilibrium water content of conventional and silicone hydrogel contact lenses. *Ophthalmic and Physiological Optics*, *26*(1), 57–64. https://doi.org/10.1111/j.1475-1313.2005.00342.x

50. Lira, M., Lourenço, C., Silva, M., & Botelho, G. (2020). Physicochemical stability of contact lenses materials for biomedical applications. *Journal of Optometry*, *13*(2), 120–127. https://doi.org/10.1016/j.optom.2019.10.002

51. Lira, M., Castanheira, E. M. S., Santos, L., Azeredo, J., Yebra-Pimentel Vilar, E., & Oliveira, M. E. (2009). *Changes in UV-visible transmittance of silicone-hydrogel contact lenses induced by wear*. https://doi.org/10.1097/OPX.0b013e318198d047

52. Glassford, S. E., Byrne, B., & Kazarian, S. G. (2013). Recent applications of ATR FTIR spectroscopy and imaging to proteins. *Biochimica et Biophysica Acta (BBA) - Proteins and Proteomics*, *1834*(12), 2849–2858. https://doi.org/10.1016/j.bbapap.2013.07.015

53. Jha, R., & Mayanovic, R. A. (2023). A Review of the Preparation, Characterization, and Applications of Chitosan Nanoparticles in Nanomedicine. *Nanomaterials*, *13*(8), Article 8. https://doi.org/10.3390/nano13081302

54. Kalam, M. A. (2016). Development of chitosan nanoparticles coated with hyaluronic acid for topical ocular delivery of dexamethasone. *International Journal of Biological Macromolecules*, *89*, 127–136. https://doi.org/10.1016/j.ijbiomac.2016.04.070

55. Danaei, M., Dehghankhold, M., Ataei, S., Hasanzadeh Davarani, F., Javanmard, R., Dokhani, A., Khorasani, S., & Mozafari, M. R. (2018). Impact of Particle Size and Polydispersity Index on the Clinical Applications of Lipidic Nanocarrier Systems. *Pharmaceutics*, *10*(2), 57. https://doi.org/10.3390/pharmaceutics10020057

56. Bhattacharjee, S. (2016). DLS and zeta potential – What they are and what they are not? *Journal of Controlled Release*, *235*, 337–351. https://doi.org/10.1016/j.jconrel.2016.06.017

57. Kayitmazer, A. B., Koksal, A. F., & Iyilik, E. K. (2015). Complex coacervation of hyaluronic acid and chitosan: Effects of pH, ionic strength, charge density, chain length and the charge ratio. *Soft Matter*, *11*(44), 8605–8612. https://doi.org/10.1039/C5SM01829C

58. Gutiérrez-Ruíz, S. C., Cortes, H., González-Torres, M., Almarhoon, Z. M., Gürer, E. S., Sharifi-Rad, J., & Leyva-Gómez, G. (2024). Optimize the parameters for the synthesis by the ionic gelation technique, purification, and freeze-drying of chitosan-sodium tripolyphosphate nanoparticles for biomedical purposes. *Journal of Biological Engineering*, *18*(1), 12. https://doi.org/10.1186/s13036-024-00403-w

59. Eaton, P., Quaresma, P., Soares, C., Neves, C., De Almeida, M. P., Pereira, E., & West, P. (2017). A direct comparison of experimental methods to measure dimensions of synthetic nanoparticles. *Ultramicroscopy*, *182*, 179–190. https://doi.org/10.1016/j.ultramic.2017.07.001

60. Pan, C., Qian, J., Zhao, C., Yang, H., Zhao, X., & Guo, H. (2020). Study on the relationship between crosslinking degree and properties of TPP crosslinked chitosan nanoparticles. *Carbohydrate Polymers*, *241*, 116349. https://doi.org/10.1016/j.carbpol.2020.116349

61. Bradu, I.-A., Vlase, T., Bunoiu, M., Grădinaru, M., Pahomi, A., Bajas, D., Budiul, M. M., & Vlase, G. (2023). Synthesis and Characterization of Polymer-Based Membranes for Methotrexate Drug Delivery. *Polymers*, *15*(21), Article 21. https://doi.org/10.3390/polym15214325